Postprint of: Makoś-Chełstowska P., Słupek E., Małachowska A., Superhydrophobic sponges based on green deep eutectic solvents for spill oil removal from water, JOURNAL OF HAZARDOUS MATERIALS, Vol. 425 (2021), 127972, DOI: 10.1016/j.jhazmat.2021.127972

Superhydrophobic sponges based on green deep eutectic solvents for spill oil removal from water

Patrycja Makoś-Chełstowska [1], Edyta Słupek [1], Aleksandra Małachowska [1]*

[1] Department of Process Engineering and Chemical Technology, Faculty of Chemistry, Gdansk University of Technology, G. Narutowicza St. 11/12, 80–233 Gdańsk, Poland;

**Correspondence: patrycja.makos@pg.edu.pl;*

KEYWORDS: deep eutectic solvents, oil-water separation, crude oil, melamine sponges

ABSTRACT: The paper described a new method for crude oil-water separation by means of superhydrophobic melamine sponges impregnated by deep eutectic solvents (MS-DES). Due to the numerous potential of two-component DES formation, simple and quick screening of 156 non-ionic deep eutectic solvents using COSMO-RS (Conductor-like Screening Model for Real Solvents) computational model was used. DES which were characterized by high solubility of hydrocarbons and the lowest water solubility were synthesized and embedded on melamine sponges. The new sponges were characterized by Fourier transform infrared spectroscopy (FT-

IR), scanning electron microscopy (SEM), X-ray diffraction (XRD), and goniometer. Several parameters affecting the crude oil-water separation (i.e. type and amount of DES, density and porosity of sponges, water contact eagle) were thoroughly studied. In order to studies of MS-DES affinity to the selected groups of crude oil i.e. Saturated, Aromatic, Resins, Asphaltenes (SARA) the thin layer liquid chromatography-flame ionization detection (TLC-FID) was used. The obtained results indicate that the melamine sponges impregnated by DES composed of eucalyptol and menthol in 1:5 molar ratio have high real crude oil absorption capacity in the range of 96.1 – 132.2 g/g and slightly depends on crude oil compositions, superhydrophobic properties (water contact angle 152°), low density of 9.23 mg/cm^3, high porosity of 99.39%, and excellent reusability which was almost not changing even after 80 cycles. The outcomes indicate that new MS-DES materials could be excellent alternatives as absorbents for the cleanup of crude oil-polluted water.

1. Introduction

During the extraction of crude oil from the bottom of the seas and oceans, as well as accidents of tankers and container ships transporting oil or its products, the leakages and the release of hydrocarbon pollutants into the sea or ocean water may occur [1]. This poses a serious safety concern for the water ecosystem [2,3]. Therefore, there is a serious challenge to clean up oil spills from the surface of the water. Typically, crude oil is removed from water using various methods i.e. in situ burning, chemical dispersants, physical sorption, air flotation, and bioremediation [4–9]. However, most of these methods have some disadvantages i.e. time and energy consumption, high cost, require complex separation steps, and cause the formation of secondary pollution. In addition, the conventional methods are not effective enough.

Currently, the physical sorption by means of porous materials has become more and more attractive oil-water separation technique due to its ability to recover and completely remove crude oil from water, without any adverse effect to the aqueous environment. So far, a number of porous materials have been tested as sorbents, i.e. zeolites, activated carbon, wood, porous polymers, clay, silicone gel, graphene aerogel [10–17]. However, some limitations still exist in these sorbent materials including poor sustainability, complicated and expensive preparation process, low selectivity, and recyclability. Ideal sorbent materials should be characterized by high oil absorption capacity, low-cost manufacturing, hydrophobicity, oleiphilicity, selectivity, and long-term reusability [18]. Recently, commercial polymeric sponges (melamine and polyurethane sponges) were considered ideal sorbents due to the low cost, high porosity structure and surface area, high absorption rate, low density, and effective mechanical properties. However, commercial sponges are characterized by hydrophilicity and oleiphilicity nature (absorb both oil and water), which prevents the effective removal of crude oil from the water [19]. Hence, surface modification of commercial sponges is the most promising method for large-scale superhydrophobic, and superoleophilic material preparation [20,21]. The superhydrophobic surface of sponges should have a water contact angle higher than 150°, and low contact angle hysteresis [22]. Superhydrophobic surface sponges can be prepared by various methods i.e. dip coating, chemical vapor deposition, in situ chemical reactions, and carbonization [21]. Among the available methods, dip coating is the most widely used for the fabrication of sponge hydrophobic surfaces. This method is simple, fast, and does not require expensive equipment, and it is consists of immersed the sponge several times in the surface-modifying agent's solution and then drying it.

The selection of solvents used for the sponge's impregnation process is a crucial parameter. The ideal solvents should be characterized by low solubility in water, high affinity to the

hydrocarbon phase, low toxicity, low cost, and easy to prepare [23,24]. Till now, polydimethylsiloxane [25], furfuryl alcohol [26], stearic acid [27], etc. were tested as hydrophobic melamine sponge coating substances. However, there is still a search for greener and perfect solvents. Until recently, due to their unique properties, ionic liquids (ILs) were considered perfect solvents. However, many problems with biodegradability, toxicity, difficult and expensive synthesis were reported which significantly limits the possibilities of their application [28–30]. Currently, deep eutectic solvents (DES) are a good alternative to ILs. DES are characterized by similar unique properties to ILs, but their synthesis is much simpler and less expensive. In addition, the application of chemical compounds from natural sources makes DES less toxic and more biodegradable than ILs. Therefore, DESs arouse much attention from both academia and industry [31]. So far they have been successfully used as extraction media [32–36] absorbents [37–41], adsorbent and polymer modifiers [42–44], lubricants [45,46], etc. However, only one paper describes studies on the sponges impregnated by DES for the removal of pesticides and dyes from water. In these studies, ionic DES composed of tetrabutylammonium bromide and fatty acids were tested as hydrophobic sponge coating [47]. To the best of our knowledge, this is the first study of the application of melamine sponges impregnated by deep eutectic solvents for the removal of model and real crude oil from water. Most of the research is based on the removal of individual substances that may be found in crude oil. Only a few works consider removing real crude oil from water. However, there are no studies in the literature that would include studies of the stability of the oil composition before and after the absorption from water. This aspect is crucial for the reuse of crude oil. In addition, there is no detailed research on the mechanisms of removing individual groups of hydrocarbons with the use of MS-based sorbents in the work published so far.

Therefore, in this paper for the first time, the detailed studies on the selection of impregnation layer of MS, explanation of the mechanism of absorption, synthesis and surface properties of new sorbets based on green DES, removal of real crude oil hydrocarbons from water, and stability of crude oil before and after absorption were described. In order to preselect DESs which have the highest affinity to the crude oil components, and the lowest affinity to water, the conductor-like screening model for real solvents (COSMO-RS) was used. Selected DES have been synthesized and used for the melamine sponges impregnation. The surface properties of new superhydrophobic sponges were determined by means of Fourier transform infrared spectroscopy (FT-IR), scanning electron microscopy (SEM), X-ray diffraction (XRD), and goniometer. All parameters affecting the crude oil removal efficiency from water (i.e. type of DES, amount of DES, time of absorption) were thoroughly optimized by means of response surface methodology (RSM) based on a central composite design (CCD). In order to deep studies of MS-DES affinity to the selected groups of crude oil i.e. Saturated (S), Aromatic (Ar), Resins (R), Asphaltenes (A) (SARA) the thin layer liquid chromatography-flame ionization detection (TLC-FID) was used.

2. Experimental section

2.1. Materials

Chemical substances for DES synthesis including camphor (C), menthol (M), thymol (Th), eucalyptol (E), octanoic acid (OA), nonanoic acid (NA), decanoic acid (DA), undecanoic acid (UDA), dodecanoic acid (DDA), citric acid (CA), 4-hydroxybenzoic acid (HA), guaiacol (Gu), and vanillin (Va) with high purity (≥ 98.0%) were purchased from Sigma Aldrich (St. Louis, MO, USA). For the preparation of model crude oil dodecane, cyclohexane, benzothiophene, dibenzanthrone, and quinolone (purity ≥ 99.0%) were purchased from Sigma Aldrich (St. Louis, MO, USA). Melamine sponges were purchased from a local supermarket in Gdansk, Poland. For

the TLC-FID analysis compressed gases such air (purity N 5.0) generated by a DK50 compressor with a membrane dryer (Ekkom, Cracow, Poland), and hydrogen (purity N 5.5) generated by Precision Hydrogen 1200 Generator (PEAK Scientific, Scotland, UK), were used. The following solvents were used to determine the group composition of crude oil dichloromethane, toluene, methanol, and hexane (purity ≥ 99.9%), which were purchased from POCH (Poland). Solvents for pretreatment of melamine sponges i.e. acetone, and ethanol (purity ≥ 99.9%), were purchased from POCH (Poland).

2.2. Real and model crude oil samples

In the studies, twelve types of model and real crude oil samples were analyzed. The samples of real crude oil came from one of the refineries in Poland. The crude oils were characterized by the various compositions of the individual hydrocarbon groups including saturated, aromatics, resins, and asphaltenes (SARA). Model crude oils were prepared by mixing substances representing individual groups in various volume proportions. In the model mixtures, dodecane and cyclohexane represented saturated compounds, pyrene - aromatic compounds, benzothiophene, quinoline - resins, and dibenzanthron - asphaltenes. The detailed compositions of the model and real crude oils are presented in Table 1.

Table 1 Composition of the crude oil samples

Crude oil samples characteristics	Abbreviation	Saturated hydrocarbons (%, w/w)	Aromatic hydrocarbons (%, w/w)	Resins (%, w/w)	Asphaltenes (%, w/w)	Density (g/cm^3) (25ºC)
Light crude oil	CO_1	70.8	24.2	4.8	0.2	0.7635
Light crude oil	CO_2	72.0	22.3	5.0	0.7	0.7945
Medium crude oil	CO_3	62.1	19.8	14.7	3.4	0.7942

Medium crude oil	CO_4	72.3	18.2	8.1	1.4	0.7245
Heavy crude oil	CO_5	39.9	24.9	30.9	4.3	0.7867
Heavy crude oil	CO_6	28.1	29	32.7	10.2	0.7914
Model crude oil	MCO_1	80	10	9.5	0.5	0.6901
Model crude oil	MCO_2	70	20	9.5	0.5	0.6960
Model crude oil	MCO_3	50	30	19.5	0.5	0.6987
Model crude oil	MCO_4	40	50	9.5	0.5	0.6997
Model crude oil	MCO_5	20	40	39	1	0.7012
Model crude oil	MCO_6	10	50	39	1	0.7019

2.3. Apparatus

The following apparatuses were used to evaluate the structural, and morphological properties of superhydrophobic sponges: Tensor 27 spectrometer (Bruker, USA) with an ATR accessory and OPUS software (Bruker, USA); scanning electron microscope FEI Quanta 250 FEG (Thermo Fisher Scientific, Waltham, MA, USA) equipped with an ET detector (Everhart-Thornley Detector, Davis, CA, USA); Rigaku Intelligent SmartLab X-ray diffraction device (Austin, TX, USA) equipped with a sealed x-ray generator; a copper shield operating at 30 mA and 40 kV, a goniometer (OCAH-200 DataPhysics, Germany). Basic physical properties of DESs and oils were measured using a DMA 4100 Density Meter (Anton Paar, Austria), BROOKFIELD LVDV-II + viscometer (Labo-Plus, Warsaw, Poland), and a cryostat (HUBER, Edison, NJ, USA). In order to analyze the group composition of crude oil before and after the absorption process, the thin layer liquid chromatography-flame ionization detection (TLC-FID) technique was used. In the studies, the Iatroscan Mk., silica gel Chromarods S5, TLC TK-8 Chromarods dryer (Iatron Lab., Japan), 3200/IS-01 semiautomatic sampler (SES, Germany), AD converter, and corresponding software (Chomik, Poland) were used.

2.4. Procedures

2.4.1. Screening of DES

In the studies, screening of 156 non-ionic deep eutectic solvents was prepared by means of the ADF COSMO-RS program (SCM, Netherlands). The geometry optimization of DES composed of two chemical compounds (menthol, camphor, thymol, eucalyptol, octanoic acid, nonanoic acid, decanoic acid, undecanoic acid, dodecanoic acid, citric acid, 4-hydroxybenzoic acid, guaiacol, and vanillin) in 1:1 molar ratio was performed using continuum solvation COSMO model at the BVP86/TZVP level of theory. For all DES the geometry optimization was performed in the gas phase to find the most stable conformers, and then vibrational analysis was performed to identify the deep eutectic solvent conformer to correspond to the true energy minimum. Only for the most energetically favorable conformer, full geometry optimization of DES was performed.

Solubility of selected crude oil components in DES (x_j) were calculated using Eq (1):

$$log_{10}(x_j) = log_{10}\left[\frac{\exp(\mu_j^{hyd} - \mu_j^{DES} - \Delta G_{j,fus})}{RT}\right] \quad (1)$$

where:

μ_j^{hyd} – chemical potential of pure hydrocarbons [J·mol^{-1}];

μ_j^{DES} – chemical potential of hydrocarbons at infinite dilution [J·mol^{-1}];

$\Delta G_{j,fus}$- fusion free energy of hydrocarbons [J·mol^{-1}];

R - universal gas constant (8.314 J·mol^{-1}·K^{-1});

T – temperature [K].

In the screening procedure, the temperature and pressure were set to be the same values as the experimental conditions i.e. 20 °C, and 101325 Pa.

2.4.2. Superhydrophobic sponges preparation and characterization

DES were synthesized by mixing two chemical compounds in 1:1 molar ratio, for which the highest affinity for the hydrocarbon phase and the lowest for the water phase were obtained during the COSMO-RS modeling stage. The synthesis was carried out at the temperature of 80°C and 1000 rpm until the homogeneous solution was obtained. Before the mixing procedure, all compounds were dried in a vacuum oven. For liquid DES, densities, and viscosity at room temperature, and melting point was determined according to the procedures from the previous studies [48]. In order to remove oxides on the surface, melamine sponges were first cleaned in ethanol and acetone using an ultrasonic bath and dried at 80°C in a vacuum oven. The sponge was cut into pieces measuring 2.5 x 2.5 x 5.5 cm. In the next step, MS have immersed in 10% DES solutions in ethanol (6 hours) and dried at 80°C for 6 hours. After this time, the DES settled evenly on all parts of the melamine sponge. The scheme of the MS-DES preparation procedure is shown in Figure 1.

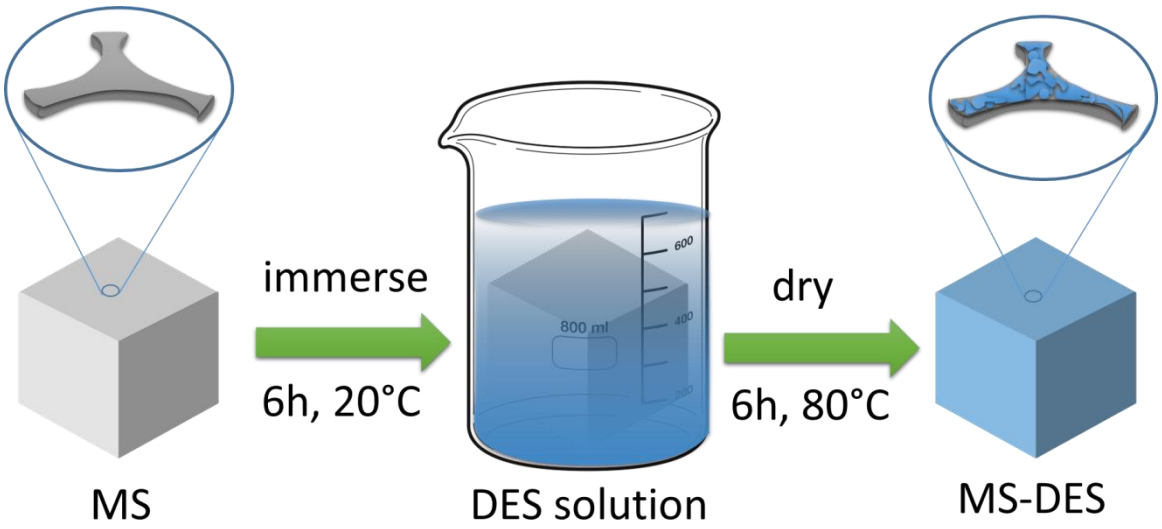

Figure 1 Schematic illustration of the MS-DES preparation.

Pure and DES impregnated melamine sponges were characterized by various techniques. The surface morphologies of MS and MS-DES were studied by means of scanning electron microscopy (SEM). The XRD was applied to confirm the chemical modifications of sponges. MS-DES were studied in the range of 5 to 80° in steps of 0.01°. The speed of sample scanning was 1°/min. The form of the sponges was determined in the vertical direction to the corresponding lattice plane. The peak with the highest intensity was used for the quantitative analysis by means of the Reference Intensity Ratio method [49]. Fourier transform infrared spectroscopy with attenuated total reflection (ATR-FTIR) analysis was used for the characterization of functional groups on the MS network. The following parameters was used: spectral range from 4000 to 600 cm^{-1}; number of background and sample scans - 256; resolution - 4 cm^{-1}; slit width - 0.5 cm. The water contact angle (WCA) of sponges was measured using a goniometer. Measurements were carried out at room temperature. The thermogravimetric analysis (TGA) of MS-DES was prepared according to previous studies [44]. The tests were conducted in pure nitrogen with a 100 mL/min flow rate in the range of temperature from 35 to 1000 °C. The temperature was increased by 10

°C/min. For each sponge sample, three measurements were made at various locations on the surfaces.

The density and porosity of MS and MS-DES were measured based on previous studies [50]. The density (ρ) was calculated using Eq. (2):

$$\rho = \frac{m_0}{V_0} \quad (2)$$

where: m_0 – mass of MS or MS-DES [g];

V_0 – Volume of MS or MS-DES [g].

The porosity (P) of sponges was calculated using Eq. (3):

$$P = \left(1 - \frac{\rho}{\rho_{bmr}}\right) \cdot 100\% \quad (3)$$

where: ρ_{bulk} – bulk melamine resin density (ρ_{bmr} = 1.51 g/cm^3).

All measurements were made in triplicate. The mean of the replicates was taken as the target value.

2.4.3. Oil-water separation procedure

The total absorption capacity test was performed by the weighing method, based on previous studies [51]. Sponges were weighed on an analytical balance, and then sponges were immersed into the crude oil. After one minute, sponges with crude oil were weighed again. Three replicates were measured for each value. The absorption capacity of sponges (ΣQ) was calculated using Eq. (4):

$$\Sigma Q = \frac{m_1 - m_0}{m_0} \quad (4)$$

where: m_1 – mass of the saturated sponge at the absorption equilibrium [g];

For the studies on the selected hydrocarbon groups' absorption capacity, the concentration of S, Ar, R, A in pure crude oil and crude oil after absorption by MS-DES and squeezing process were measured using TLC-FID based on standard test method IP 469/01 [51]. The absorption capacity for selected hydrocarbons (Qi) were calculated using Eq. (5):

$$Q_i = \frac{C_1 - C_0}{C_0} \quad (5)$$

where: C_1 – Selected hydrocarbons group concentration in raw crude oil [%];

C_2 – Selected hydrocarbons concentration in crude oil after sponge squeezing [%].

After the absorption process, the reusability of MS-DES was studied by repeated absorption-desorption gravimetric measurements consisting of 50 runs, based on the previous studies In all cycles, the DES-MS was immersed in 50 mL of crude oil (model and real) for 60 sec. and weighted, and then squeezed to extract the absorbed crude oil. The desorption efficiency (R) was calculated by the following Eq. 6.

$$R = (1 - \frac{m_3}{m_1}) \cdot 100\% \quad (6)$$

Where: m_3 - mass of the MS-DES after manual squeezing [g].

2.4.4. Central composite design

The most important independent variables including time of immersion sponge in crude oil, the concentration of DES in impregnation solution, and HBA:HBD molar ratio was used for the optimization of the real and model crude oil absorption condition. In this proposal, a central composite design model was used. The variables were studied at five different levels including -1.68, -1, 0, 1, and 1.68. The model plan was composed of 20 runs. All experiments were repeated

in triplicate. In order to prediction of the optimal point of crude oil absorption capacity, the second-order polynomial model was fitted, to correlate the independent variables. Equation (7) of the quadratic model was used to predict dependent variables:

$$Y_k = \beta_0 + \sum_{i=1}^{3} \beta_i \cdot X_i + \sum_{i=1}^{3} \beta_{ii} \cdot X_i^2 + \sum_{i=1}^{3} \beta_{ij} \cdot X_i \cdot X_j \quad (7)$$

where: Y_k - predicted dependent variables (real and model crude oil);

β_0 – intecept;

β_i - linear model coefficient;

β_{ii} - quadratic model coefficient;

β_{ij} - interaction model coefficient;

X_i, X_j - independent variables ($i \neq j$).

3. Results and discussion

3.1. Screening of DES

In the studies, screening of 156 non-ionic deep eutectic solvents composed of terpenes (i.e. menthol, camphor, thymol, eucalyptol), carboxylic acids (i.e. octanoic acid, nonanoic acid, decanoic acid, undecanoic acid, dodecanoic acid, citric acid, and 4-hydroxybenzoic acid), and phenols (guaiacol, and vanillin) was prepared by means of the COSMO-RS model. The model included DES in which all the substances mentioned were mixed with each other in a molar ratio of 1:1. The solubility of individual hydrocarbons in DESs, and the lack of water solubility in DESs were chosen as criteria for selecting the best DESs. Among the studied solvents, DES composed of citric acid, and 4-hydroxybenzoic acid, vanillin and guaiacol show high water solubility (higher than 2000 g/L), which is due to the high solubility of individual substances in water. The results indicate that these DES will not be able to form hydrophobic coatings on the surface of melamine

sponges. The lowest calculated water solubility represents complexes which were form from almost insoluble or slightly soluble substances in water i.e. menthol (0.4 mg/L), camphor (1.2 mg/L), thymol (0.9 g/L), eucalyptol (3.5 g/L), octanoic acid (0.68 g/L), nonanoic acid (0.3 g/L), decanoic acid (0.15 g/L), undecanoic acid (0.023 g/L), dodecanoic acid (0.015 g/L). The second criterion was affinity of selected hydrocarbons to DES. The results indicate that dodecane and cyclohexane which represent saturated hydrocarbons in model crude oil have the highest solubility (<2000 g/L) in DES composed of all terpenes and linear carboxylic acids. In addition, vanillin with linear carboxylic acids, and terpenes combination show similar dodecane, and cyclohexane solubility. For the pyrene which represents aromatic components, benzothiophene (resins), and dibenzanthrone (asphalenes), the similar results were obtained. The only quinoline showed high solubility in all tested DES (Figures 2, and S1).

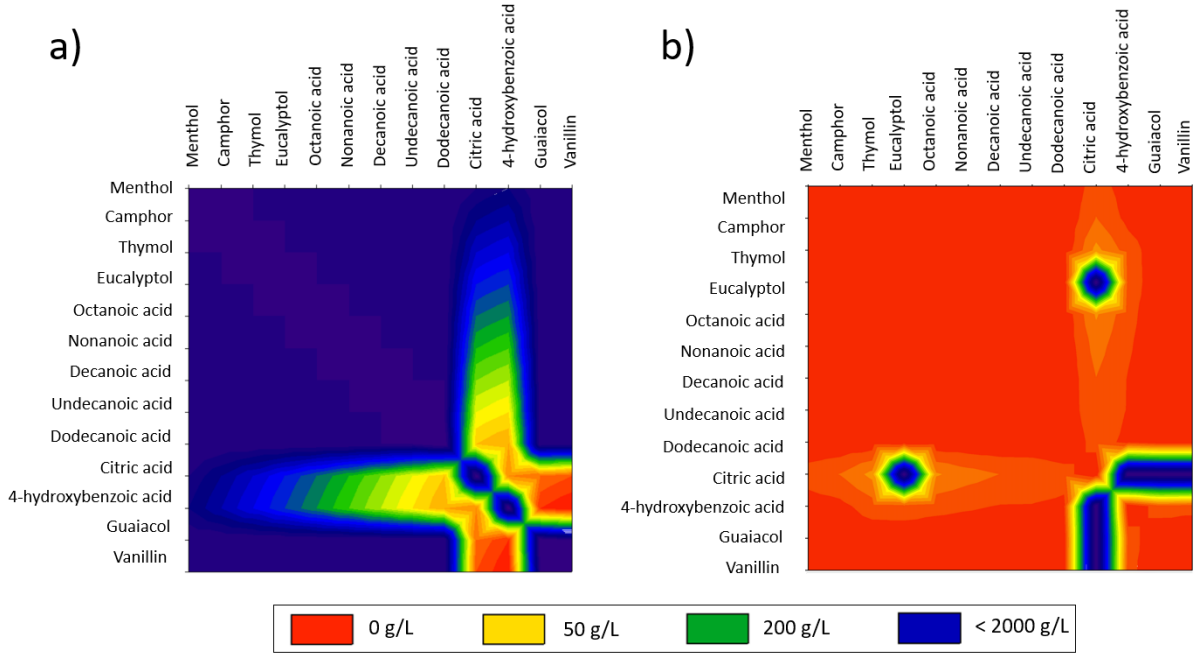

Figure 2 Solubility screening of a) dodecane, and b) water in various deep eutectic solvents complexes in 1:1 molar ratio.

In order to explanation of the hydrocarbons and water affinity to DES and interpret the interaction between molecules, the charge-related σ-profiles were applied based on the previous studies [37,40]. The σ-profile is one of the most important molecule-specific properties, which can be defined as the probability distribution of surface area with charge density (σ) [52]. In the studies, σ-profiles were present as two histograms, one represents DES components (Figure 3a) and the second – water and selected hydrocarbons (Figure 3b). Both histograms were divided into three regions including hydrogen bond donor (HBD) region in range of $\sigma < -0.0084$ e/Å^2, non-polar region in range of -0.0084 e/Å$^2 < \sigma < 0.0084$ e/Å^2, and hydrogen bond acceptor (HBA) region in $\sigma > 0.0084$ e/Å^2 range. The obtained results show that all the DES components have the highest peak in the non-polar region (nonhydrogen bond region). Smaller peaks can be identified in the areas responsible for the HBA and HBD properties of DES. From the DES components, camphor and eucalyptol have only a small peak in the HBA area, and there is no peak in the HBD area. This is due to the fact that in their structures only ether (–O–), and carbonyl (=O) groups occur. This indicates that both components play a role as HBA, and there is no possibility of DES formation by mixing each other. Menthol and thymol can be classified to the HBD group of compounds, due to the visible peak in the region below $\sigma < -0.0084$ e/Å^2, and lack of peak in $\sigma > 0.0084$ e/Å^2 region. Both components contain hydroxyl group (-OH) which are able to the formation of strong H-bonding. Theoretically, linear carboxylic acids including octanoic acid, nonanoic acid, decanoic acid, undecanoic acid, and dodecanoic acid, due to the carboxylic group (-COOH) also should have only one peak in the HBD region. However, a small peak can also be observed in the HBA region. This indicates that carboxylic acids can play both roles as HBA and HBD components. Therefore, they can form DES by mixing with each other and form hydrogen bonds. The rest of the DES components including citric acid (-COOH, and –OH), 4-hydroxybenzoic acid (-COOH,

and –OH), vanillin (-O-CH_3, -CHO, and -OH), and guaiacol (-O-CH_3, and –OH) also can play both HBA and HBD role in DES formation. From the model crude oil components, none of them showed a peak in the HBD range. The only dibenzanthron which have carboxylic group, as well as quinoline and benzothiophene which have heteroatoms in their structures show a small peak in the HBA region and a large peak in the non-polar region. The rest of the crude oil components including cyclohexane, dodecane, and pyrene have the only peak in the range in the range of $-0.0084\ e/Å^2 < \sigma < 0.0084\ e/Å^2$ regions. The chart of water indicates that molecules contain only peaks in HBA, and HBD region, and don't have the peak in the non-polar area.

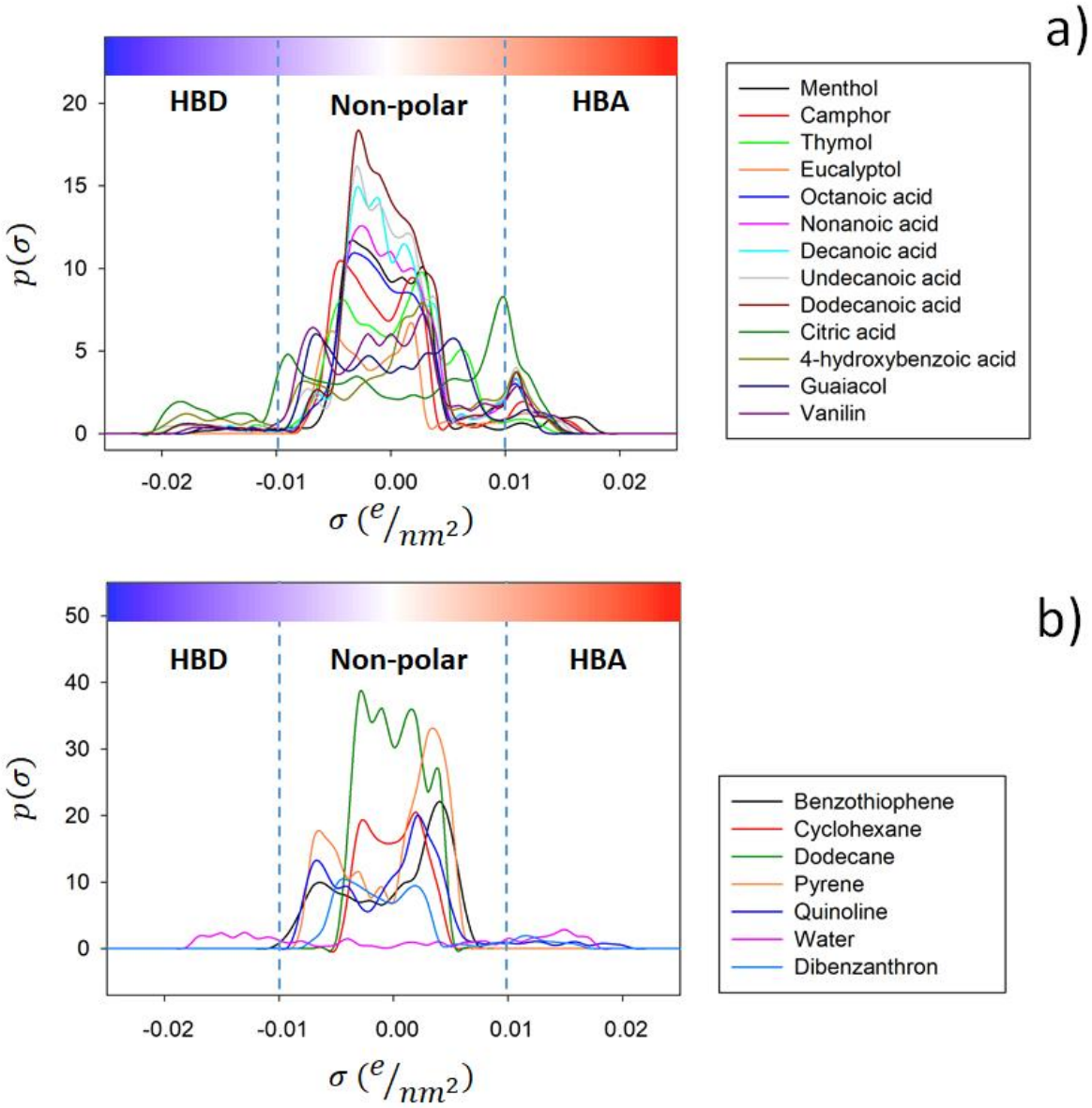

304

305 **Figure 3** Sigma profile of a) DES components; b) model crude oil components generated through
306 COSMO-RS model.

307 In order to the identification of the localization of active groups in DES and model crude
308 oil components, studies of electrostatic potential (ESP) analysis was performed. Figures 4 and 5
309 show the ESP of components that are mapped onto electron densities. The blue area on each
310 component represents positive potential regions, the red area indicates the negative potential, and

311 the white shows a non-polar region in which the potential region is close to zero. In all studied
312 components, the electropositive area is located around the hydrogen atoms in –COOH, –OH, and
313 –CH, $–CH_2$, and $–CH_3$ groups. The nonpolar region is located around carbon atoms, and the
314 electronegative area is located close to the oxygen, sulfur, and nitrogen atoms in –O–, –S–, and –
315 N– groups. During deep eutectic solvents' formation, the electropositive region from one of the
316 compounds attracted the electronegative area of the second chemical compound. Then a non-
317 bonded interaction (i.e. H–bonding) formed between the active groups of DES compounds. These
318 interactions are responsible for the formation of stable DES structures with much lower melting
319 points compared to the pure components. The same interactions also are formed during the
320 attachment of DES to crude oil components. Among the crude oil components, particularly strong
321 interactions with DES should be visible for quinoline, benzothiophene, and dibenzanthrone, due
322 to the presence of active groups, i.e. -N-, -S- and = O in their structures. For the remaining
323 components of the model crude oil, i.e. pyrene, cyclohexane, and dodecane, only weak red and
324 blue surfaces can be observed. This indicates that a weaker, non-bonded interaction will form
325 between DES and the hydrocarbons.

326

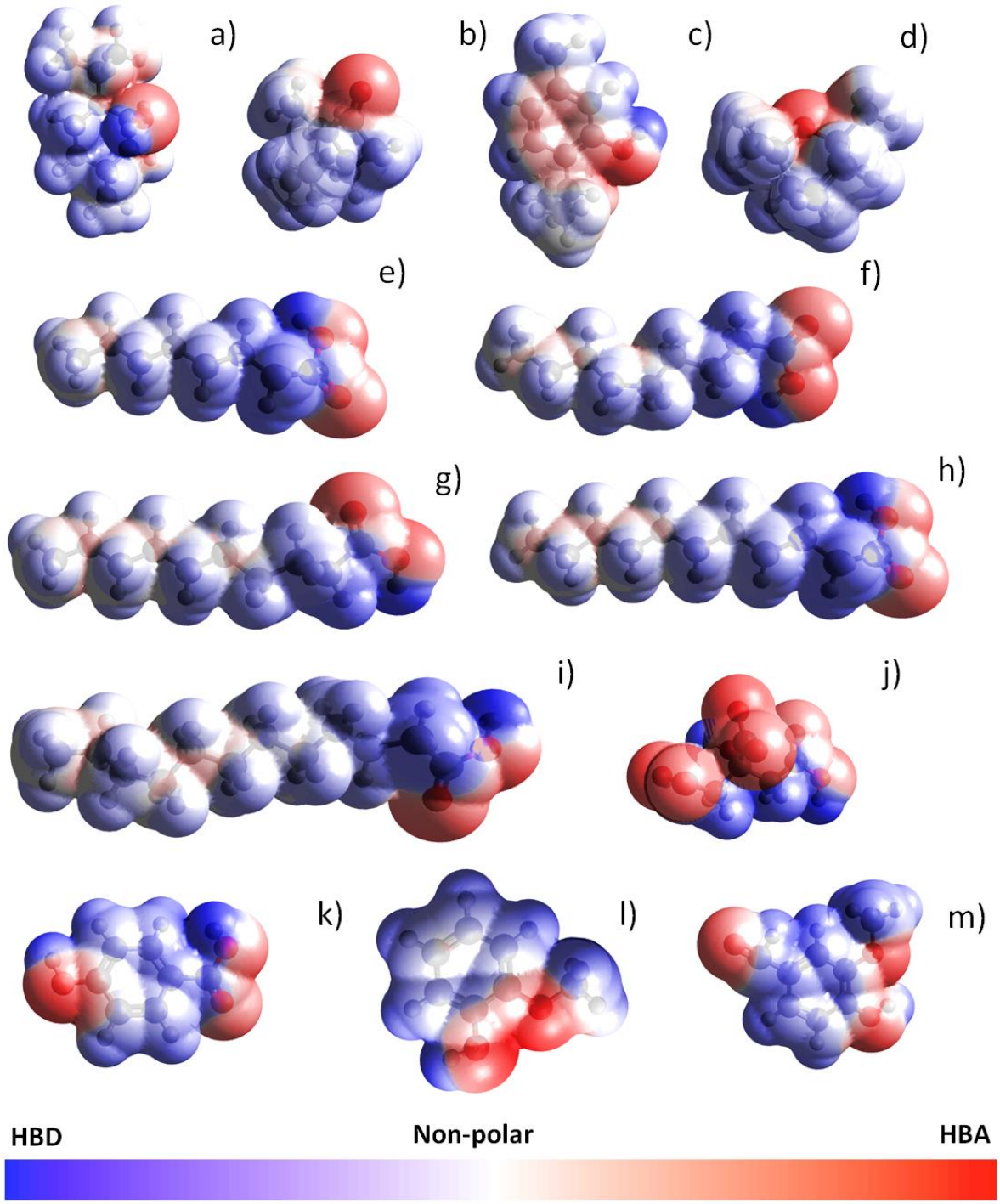

Figure 4 Electrostatic potential maps of DES components: a) menthol, b) camphor, c) thymol, d) eucalyptol, e) octatonic acid, f) nonanoic acid, g) decanoic acid, h) undecanoic acid, i) dodecanoic acid, j) citric acid, k) 4-hydroxybenzoic acid, l) guaiacol, m) vanillin.

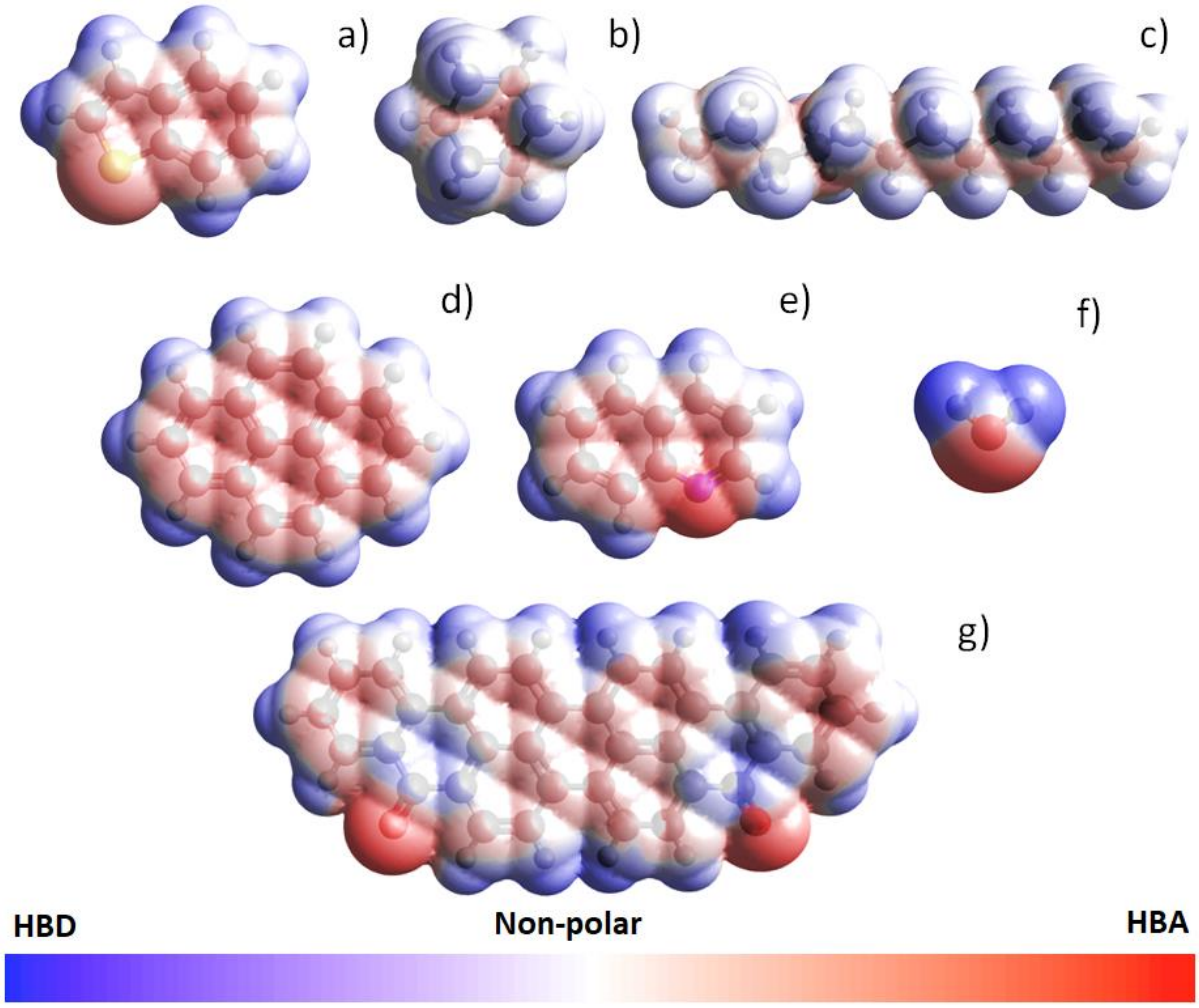

Figure 5 Electrostatic potential maps of water and model crude oil components: a) benzothiophene, b) cyclohexane, c) dodecane, d) pyren, e) quinoline, f) water, and g) dibenzanthron.

3.2. DES formation and characterization

Based on the COSMO-RS results, only DES which is characterized by high affinity to the hydrocarbons phase and low affinity to the water phase was synthesized. Therefore, only terpenes and carboxylic acids were mixed with each other in a 1:1 molar ratio. Some synthesized DES have already been published. Therefore, basic physical properties (i.e. density, viscosity, and melting point) which can be affected oil-water separation were studied only for the new DES. All physical

data of studied DES (published and new) are presented in Table S1. The obtained results indicate that not all of the 36 proposed two-component complexes form deep eutectic solvents. The melting point of M:UA, M:DDA, C:E, C:DDA, Thy:DDA, OA:DDA, NA:DDA, DA:DDA is higher than 25 °C. In the combinations of most of the studied mixtures of monoterpenes with fatty acids, a trend can be observed that with the increase in the length of the aliphatic chain in the acid structure, the melting point increases. Most monoterpenes in combination with DDA acid have a melting point above room temperature. Only eucalyptol forms a eutectic mixture with DDA, the MP of which is 8.5°C. In addition, some monoterpene mixtures also do not form eutectic liquids, i.e. eucalyptol and camphor. This is due to the fact that both components have active oxygen atoms in their structures, which are good acceptors of hydrogen bonds. Nevertheless, the structure of the molecules lacks hydrogen bond donors, which prevents the formation of strong bonds between the components. This is confirmed by the previous considerations.

In most processes, the viscosity of solvents should be low as possible to ensure fast process kinetics. It is in line with Walden's rule that the lower the viscosity, the greater the diffusion coefficients, and vice versa. If the viscosity is too high, the mass transfer process is slow and ineffective [53]. On the other hand, higher viscosity can more easily trap DES in the pores of the sponge and stay longer on the sponge surface. However, this can lead to clogging of the pores and reduce the absorption space, and limited the absorption capacity. Therefore, low-viscosity DES should be chosen for the impregnation of sponges. The viscosity of the tested DESs at 25 °C is in the range from 4.4 to 57.9 mPas. The lowest viscosity was obtained for DES composed of eucalyptol. These values were 8.04, 5.25, 5.89, 6.37, 6.8, and 7.16 for E:M, E:OA, E:NA, E:DA, E:UDA, and E:DDA, respectively.

The next important DES physicochemical parameter is density. The fact that petroleum hydrocarbons and crude oil have a lower density than water causes them to float on the surface of the water. Therefore, the new DES, which will be used for impregnation, should not have higher densities so as not to flood the sponge. The obtained results of the density of DES indicate that all densities are lower than water. DES densities are in the range of 0.8362 – 0.9873 g/cm^3. It can be concluded that all DES fulfill the necessary condition of low density.

3.3. Superhydrophobic sponges preparation and characterization

3.3.1. MS-DES characterization, and pre-selection

Only DESs, which were liquids at room temperature, were deposited on melamine sponges. All prepared MS-DES were analyzed with a goniometer to determine the contact angle for water and real crude oil samples. In addition, the density and porosity tests for all the MS-DES were prepared. For preliminary tests, medium real and model crude oil samples (CO_3, and MCO_3) which represent the most popular crude oils composition were used. The obtained studies indicate that all the prepared MS-DES are characterized by hydrophobicity character. The WCA of all sponges was higher than 125° (Figure 6). This is due to the hydrophobic nature of pure DES. Additionally, such results indicate a very thorough impregnation of the melamine sponges. On the other hand, the contact angle of both model and real crude oil was 0° for all 25 MS-DES. This indicates a very good oil absorption capacity of the impregnated sponges. The pure melamine sponge showed high wettability for both water and crude oil, which indicates a hydrophilic and oleophilic character. In both cases, the contact angle was 0°. The density and porosity of sponges are also important parameters that decide the absorption capacity of MS-DES. Theoretically, the greater the porosity and the lower the density, the greater the absorption capacity. The density and porosity of pure MS were 8.72 mg/cm^3, and 99.42%, respectively. All sponges were less porous

than pure sponges. Among the impregnated sponges, MS-E:M was characterized by the highest porosity (99.32 %), and the lowest density (10.26 mg/cm^3). Slightly lower porosity was found for the remaining sponges impregnated by DES composed of menthol. The porosity values were 98.07, 98.17, 97.29, and 95.21 % for MS-M:Th, MS-M:OA, MS-M:NA, and MS-M:DA, respectively. These sponges were also characterized by low density. The lowest values of porosity in the range of 81.84 - 93.47% and the highest density in the range of 98.6 – 274.2 mg/cm^3 were obtained for MS impregnated with DES composed only of carboxylic acids. The reduced porosity and higher density of impregnated sponges result from the uneven distribution of DES on the surface of the sponges, as well as from the clogging of the pores by DES, which prevents the penetration of crude oil into the sponges [54].

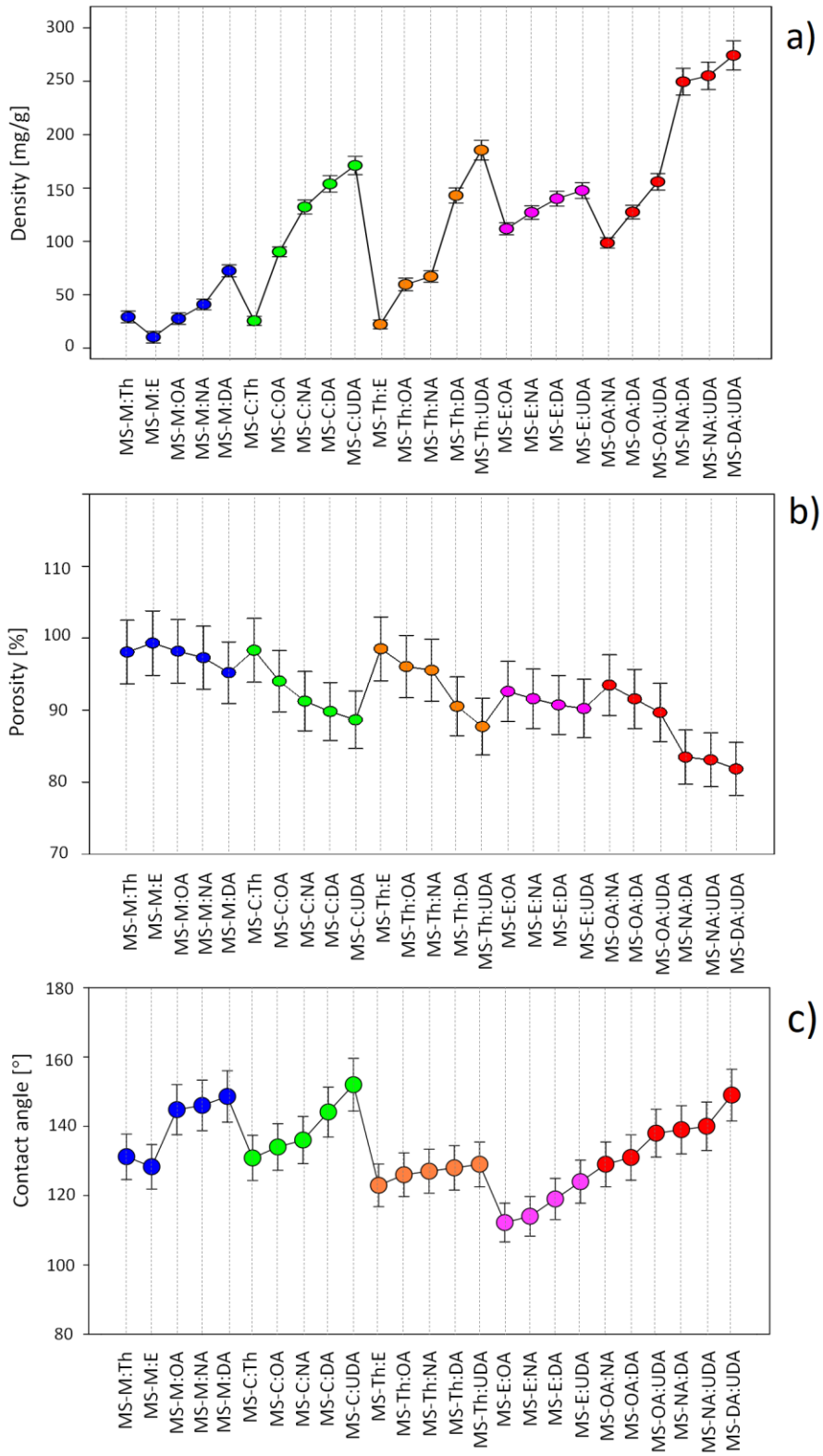

396

397 **Figure 6** Density, porosity and water contact angle of MS-DES.

In the next part of the studies, the tests of the model and real crude oil absorption capacity were prepared. The obtained results indicate that the MS-E:M and MS-M:Th sponges have the highest absorption capacity, with 97.5 g/g, and 81 g/g capacities values. For the remaining sponges, the values did not exceed the capacity of 50 g/g. Similar results were obtained for model crude oil. The same sponges i.e. MS-E:M, and MS-M:Th were characterized by the highest absorption capacity (112.7 and 83.6 g/g). The results are presented in Figure 7. For a clean sponge, the results of the absorption capacity were very similar to MS-M: E. However, due to the hydrophilic nature of pure MS, it cannot be used to remove oil from water. Therefore, in further studies, only sponge MS-E:M (1:1) which is characterized by hydrophobicity, high porosity, low density, and high absorption capacity of both model and real crude oil were used.

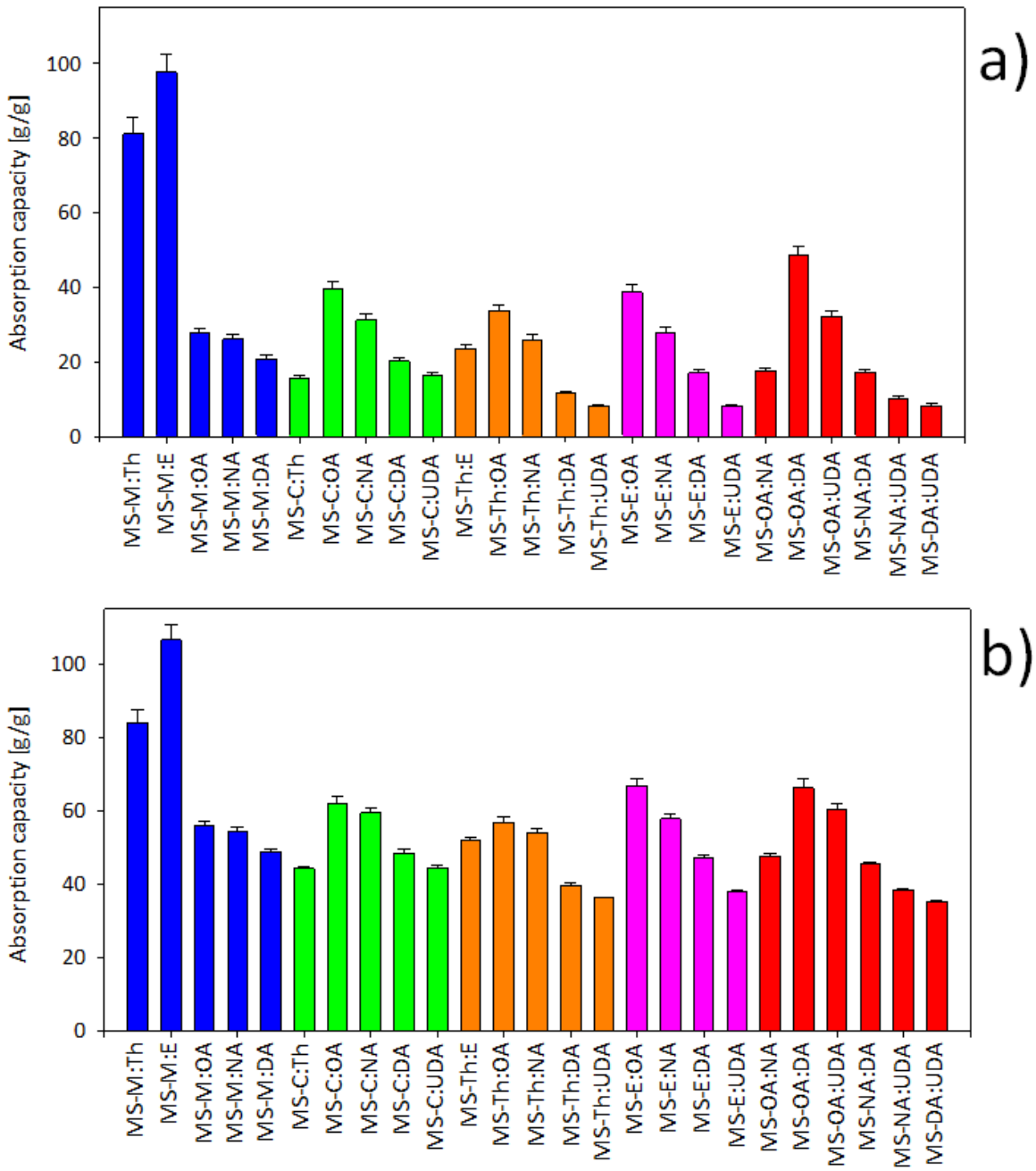

408

409 **Figure 7** Absorption capacity of a) real, b) model crude oil by melamine sponges embedded by

410 DES (MS E:M (1:5)).

411

412

413

3.3.2. SEM analysis

In the further part of the studies, the DES composed of menthol and eucalyptol were also prepared in 1:2, 1:3, 1:4, and 1:5 molar ratios, and then they were used to impregnate the sponges. The morphology of the sponges before and after DES impregnation (MS, MS-E:M (1:1), MS-E:M (1:2), MS-E:M (1:3), MS-E:M (1:4), and MS-E:M (1:5)) was studied by Scanning Electron Microscopy with Energy Dispersive X-Ray Analysis (SEM-EDX) measurements. The SEM results are presented in Figures 8 and S2. Figure 8 shows that the melamine sponge before impregnation is characterized by a three-dimensional, hierarchical, and porous structure with a pore size of approx. 80-100 μm and smooth skeleton surface with a diameter of approx. 10 μm. After the impregnation process, the sponges did not change their porous structure (Figure 8, and S2). A slight increase in the diameter of the skeleton can be observed, which indicates a DES-impregnated layer. The pores are not blocked, which is beneficial for the absorption and increased flow of hydrocarbon substances [55]. Additionally, the skeleton surface has become rough after the impregnation process and fine particle clusters can be observed. The particle clusters and thin film on the skeleton surface are responsible for the hydrophobic and oleophilic nature of the sponges.

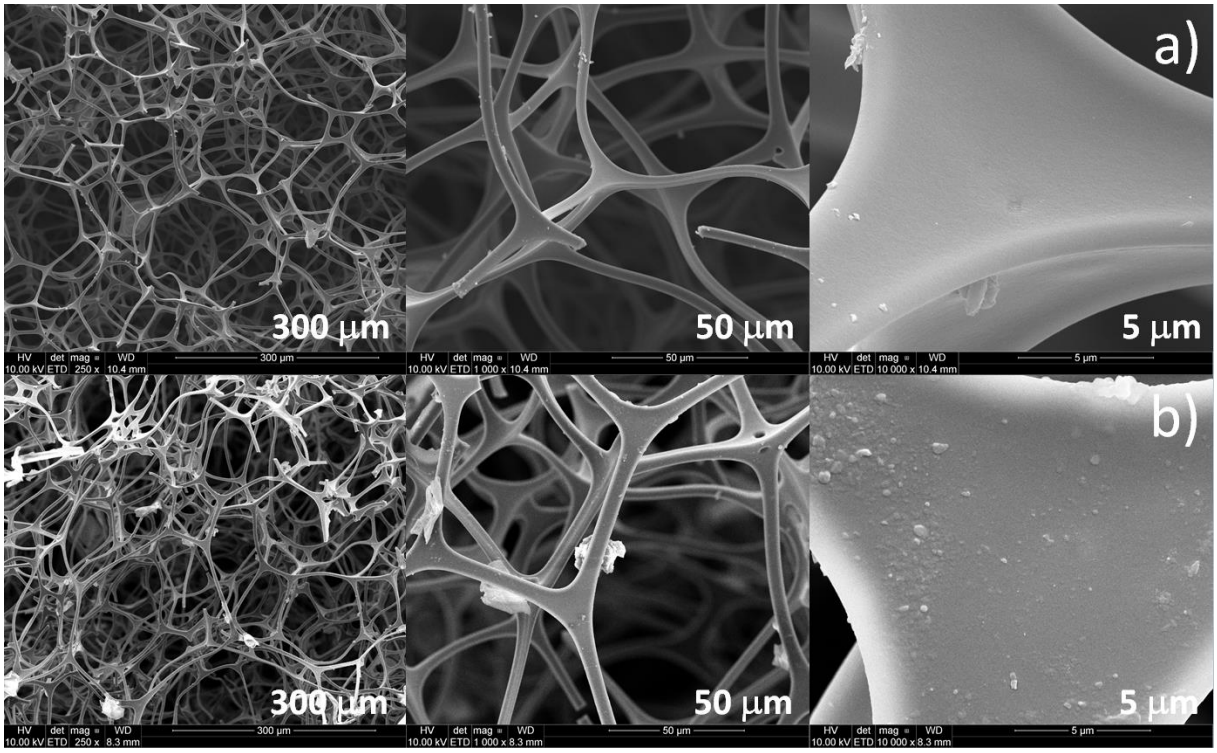

Figure 8 SEM images of a) pure MS, and b) MS-E:M (1:5).

The elemental composition of the sponges was studied with EDS. The results of pure MS and MS-E:M (1:5) are presented in Figure 9. The pure MS sponge contains only C, N, and O atoms, which is in line with the standard composition of melamine foam [60,61]. In the sponge, after the MS-E:M (1: 5) impregnation process, an increase in the ratio of carbon and oxygen to nitrogen atoms can be observed. This is due to the presence of a DES layer on the surface of the MS skeleton. Similar results were obtained for the remaining sponges (MS-E:M (1:1), MS-E:M (1:2), MS-E:M (1:3), and MS-E:M (1:4)).

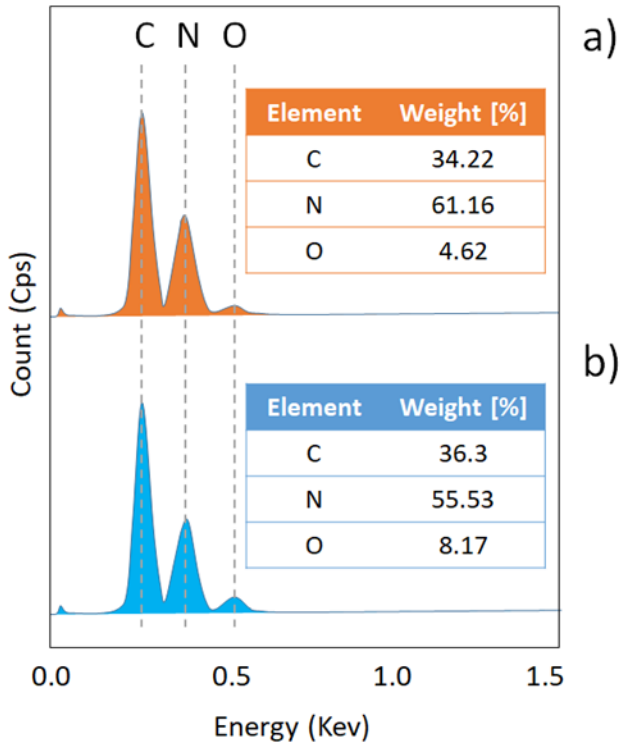

440

441 **Figure 9** Element compositions of a) pure MS, and b) MS-E:M (1:5).

442 3.3.3. XRD analysis

443

444 The microstructures of sponges were studied by XRD analysis. The diffractograms of pure MS

445 and MS after impregnation in the 2θ interval ranging from 5 to 80° are presented in Figure 10. It

446 can be seen that pure MS and all MS-DES present broad peak in the range of 10 – 30 °C which

447 suggest the non-crystalline nature of melamine sponges. According to the literature data, if the

448 sponges had a crystalline form, then in the diffractogram peaks around 17.4, 20.6, 25.3, 30.6, 31.6,

449 33.6, 34.8, and 44.9° can be observed [56].

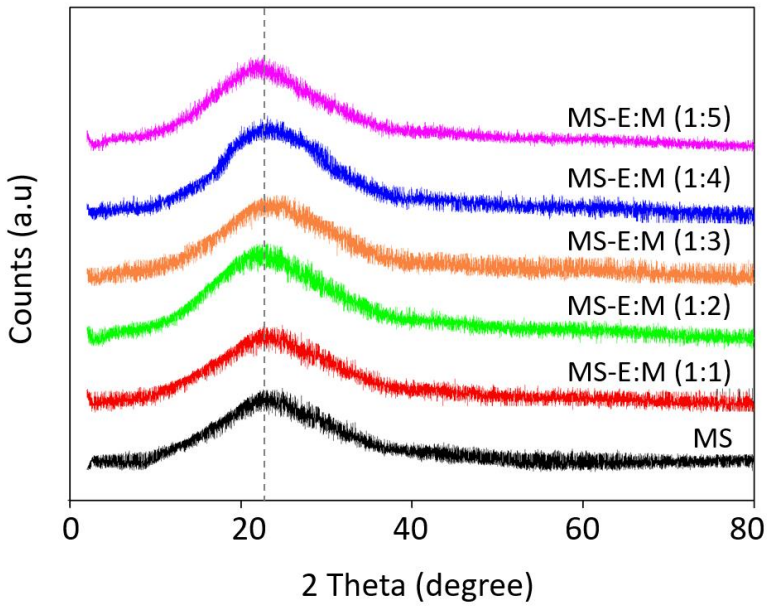

Figure 10 XRD diffractograms of pure MS, and MS after DES impregnation MS-E:M (1:1), MS-E:M (1:2), MS-E:M (1:3), MS-E:M (1:4), and MS-E:M (1:5).

3.3.4. FT-IR analysis

For understanding the intermolecular interactions between DES and sponges, ATR-FTIR spectroscopy was applied. All spectra are presented in Figure 11. In the spectrum of pure melamine sponge, prominent peaks at 3357, 1512, 998, and 812 cm^{-1} can be observed. These peaks can be assigned to N – H stretching of the primary and secondary amines, C – N stretching, C – O stretching, and s-triazine ring bending, respectively. The peaks in 1310, and 998 cm^{-1} indicate the C−H bending. In addition, two peaks with low intensity can be observed at 2891 and 2827 cm^{-1} which can be attributed to C−H stretching [57–60]. All identified peaks in the MS spectrum remained at the same positions in the spectra of the sponges after DES impregnation. On the other hand, the peak of the N-H group was covered with the peak of the -OH group of menthol. However, based on previous research, the N-H group should participate in the formation of hydrogen bonds with DES components [26]. In the spectra of MS-DES, the most intense peaks come from the DES

components. The peaks in range from 2951 to 2868 cm^{-1} corresponds to the symmetric and asymmetric CH_2 and CH_3 stretch. The lower intensity peaks at 2920 and 2871 cm^{-1} can be attributed to a methyl group. A broad peak corresponding to a hydroxyl group (–OH) is observed at 3347 cm-1 in MS-E:M (1:1) and MS-E:M (1:2). As the menthol content in DES increases, a shift of the peak towards lower values can be observed. Similar behavior was observed for the peak located at 1025 cm-1 which is attributed to the C-O bond. This indicates the –OH group is involved in the formation of hydrogen bonds between M and E, and between M and MS.

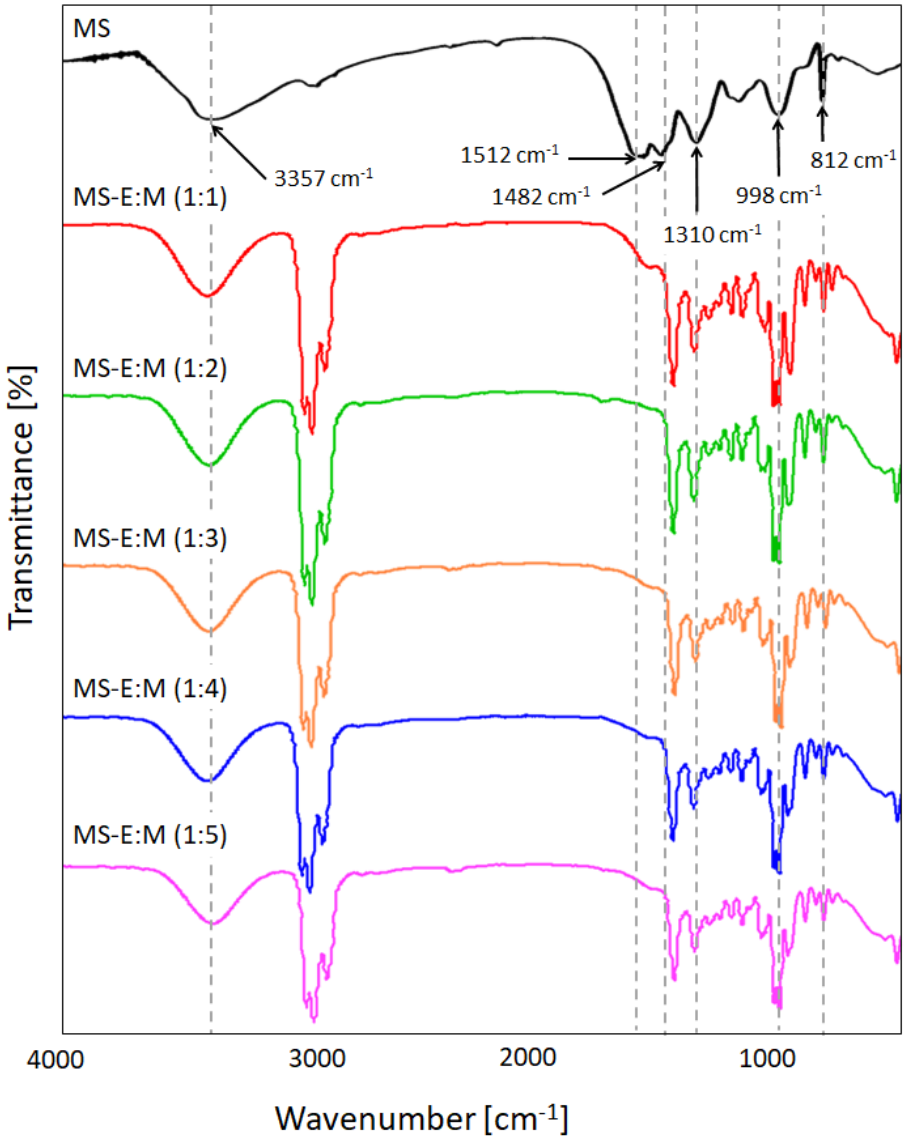

473 **Figure 3** ATR-FTIR spectra of pure MS and MS after DES impregnation.

474 3.3.5. Water contact angle, density, and porosity of MS-M:E

475

476 The results of the densities of MS-E:M in various molar ratios, indicate that as the menthol
477 content in DES increases, the MS-DES density gradually decreases, from 10.58 to 9.23 mg/cm^3.
478 The opposite results were obtained for porosity, which is closely related to density. The porosity
479 increased from 99.3% to 99.39%. However, in the case of both parameters, the changes are
480 insignificant and are within the standard deviation. They can be considered statistically

insignificant. The most important and the greatest change can be observed for the WCA parameter. As the menthol content in DES increased, the contact angle increased from 126° to 152°. The obtained results indicate that after increasing the E:M molar ratio to 1:5, the MS began to fulfill the criteria of a superhydrophobic surface. This is due to the fact that menthol, characterized by lower water solubility than eucalyptol. On the other hand, the crude oil contact angle did not change with increasing menthol content in DES, and for each of the crude oil samples were 0°. These results are also confirmed by the fact that the sponge without modification begins to fall to the bottom of the beaker immediately after being immersed in water, while the sponge impregnated with DES floats on the surface of the water. When both types of sponges with and without impregnation layer were immersed into the beaker with water and crude oil, then both sponges begin to absorb the oil and sink to the bottom of the beaker. This indicates that the clean sponge is hydrophobic and oleophilic, while the modified DES sponge has oleophilic character and excellent water-repelling properties. Similar results were also observed for MS impregnated by furfuryl alcohol, have the WCA 138–145° [26]. All obtained results are presented in Figure 12.

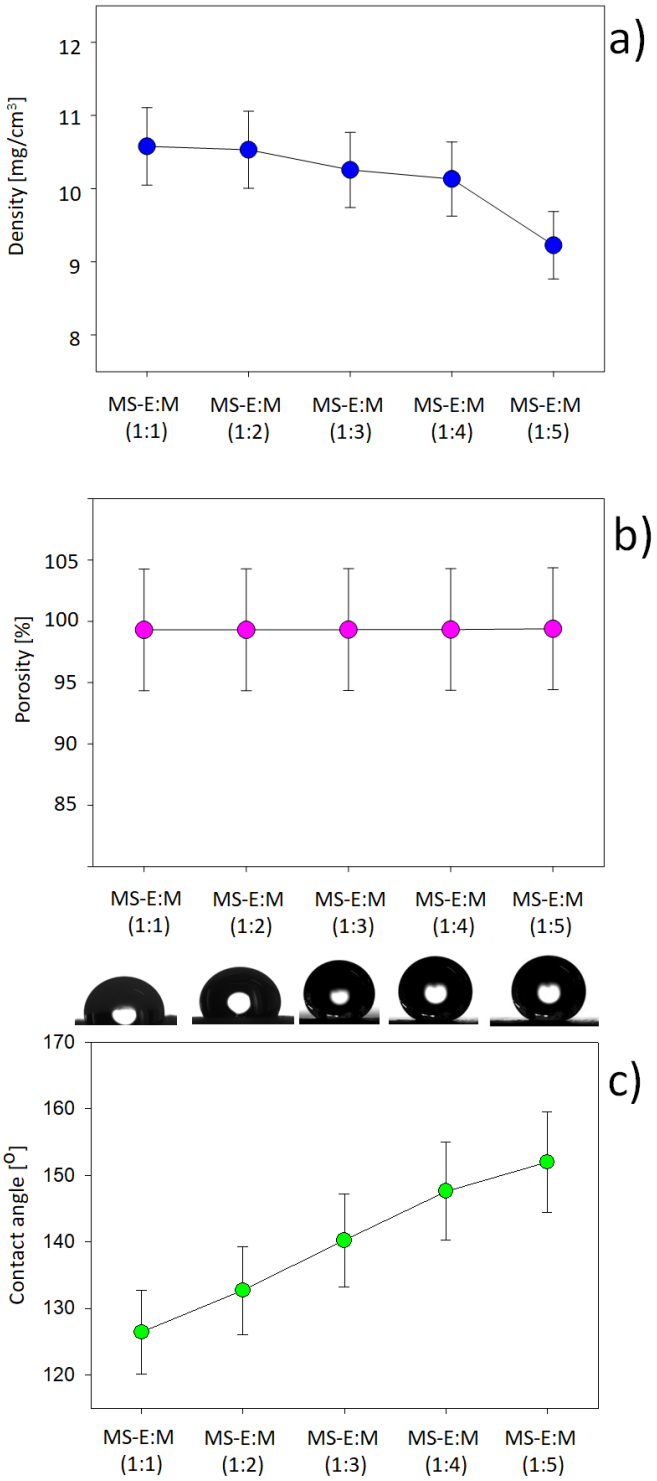

Figure 4 Density, porosity, and water contact angles of impregnated sponges MS-E:M (1:1), MS-E:M (1:2), MS-E:M (1:3), MS-E:M (1:4), and MS-E:M (1:5).

3.4. Optimization of MS-DES parameters

3.4.1. Central composite design

In further studies, the MS-DES which represents the highest crude oil absorption capacity was used in the CCD model. For MS-M:E, the most important parameters were applied to plan a subsequent higher order 2^2 design. Three factors including DES concentration, HBA:HBD molar ratio and time of immersion in the mixture of crude oil-water were used for the optimization. In Table 2 the extended values for all the parameters in five levels are presented. The design matrix and responses for absorption capacity of real and model crude oil are presented in Table S2.

Table 2 Experimental ranges and levels of two variables in CCD.

Variables	**Ranges and levels (star points = $(2^k)^{1/4}$= 1.682) [a)]**				
	-α	**-1**	**0**	**+1**	**+α**
(X_1) DES concentration [%, w/w]	4	8	14	20	24
(X_2) HBA:HBD molar ratio	1:1	1:2	1:3	1:4	1:5
(X_3) time of immersion [s]	3.2	10	20	30	36.8

[a)] *k – number of variables = 3*

In order to identify the most important effects and interactions, analysis of variance (ANOVA) was used. The results of ANOVA tests are presented in Table S3-S4. In the studies, values of typical parameters i.e. F- and p-values were adopted as the criteria at a 95% confidence level. The ANOVA results for both model and real crude oil indicate that in the linear parameters, the effects of the prominent variables are significant on response, with p-values < 0.05. Similar results were obtained in the quadratic parameters. Only for $X_3 \cdot X_3$ the p-value was higher than 0.05. The obtained response levels of the interactions of independent variables indicate that in both types of

samples, the relationship between DES concentration and HBA:HBD molar ratio had the greatest impact on the model (p-value < 0.05). In addition, the p-value of both models was found to be statistically significant due to the p-value <0.0001, and F-values equal to 49.58 and 45.55 for real and model crude oil samples respectively. The lack of fit relative to the pure error was considered insignificant due to the p-value of 0.121 and 0.101 for real and model crude oil, respectively.

The obtained experimental response equations results of real and model crude oil can be expressed as follow (Eq. 6-7):

$$\text{Real crude oil: } Y_{QR}\,[g/g] = -101.1 + 32.24\,X_1 + 5.15\,X_2 + 0.678\,X_3 - 1{,}762\,X_1 \cdot X_1 - 0{,}0999\,X_2 \cdot X_2 - 0{,}001221\,X_3 \cdot X_3 - 0{,}811\,X_1 \cdot X_2 - 0{,}0561\,X_1 \cdot X_3 + 0{,}01234\,X_2 \cdot X_3 \quad (6)$$

$$\text{Model crude oil: } Y_{QM}\,[g/g] = -120 + 36.6\,X_1 + 5.91\,X_2 + 0.851\,X_3 - 1.897\,X_1 \cdot X_1 - 0.1079\,X_2 \cdot X_2 - 0.001700\,X_3 \cdot X_3 - 0.932\,X_1 \cdot X_2 - 0.0693\,X_1 \cdot X_3 + 0.01176\,X_2 \cdot X_3 \quad (7)$$

where: Y_{QR} and Y_{QM} - absorption capacity of real and model crude oil;

X_1, X_2, and X_3 - independent variables.

In both models high determination (R^2), predicted (R_{pred}^2), and adjusted (R_{adj}^2) coefficients were obtained. For the real crude oil model the following values were obtained R^2 = 97.81%, R_{pred}^2= 85.78%, R_{adj}^2= 95.84%, while for the model crude oil the results were as follows: R^2 = 97.62%, R_{pred}^2= 84.48%, R_{adj}^2= 95.45%. The determination coefficient values indicate that in the models there is a good correlation between the experimental results, as well as a good fit of the model and the possibility of predicting the results for new batch data.

In both models all parameters i.e. DES concentration (X_1), HBA:HBD molar ratio and time of immersion (X_3) show the significant linear effect on the absorption capacity of real and model

crude oil, due to the p-value below 0.05. Furthermore, from the interactive effects of parameters, the DES concentration and HBA:HBD molar ratio is also significant (p-value equal 0.002 for both model and real crude oil models).

HBA:HBD molar ratio of impregnated DES is one of the most important parameters which decide to efficient absorption of hydrocarbons phase and low water absorption. Based on Figures 13 and S3 It can be conducted that with the increase of the menthol content in DES structures, the absorption capacity of MS-DES increases. This is probably due to the fact that menthol has –OH group in the structure, which can attract many petroleum compounds containing –CH-, -CH_2- and CH_3 groups, and heteroatoms, i.e. N, S, and O, and for with it strong bonding. Additionally, as observed in point 3.3.5. With the increase in menthol content in DES structures, the WCA increases. This indicates that the MS-E:M (1:5) allows the selective absorption of crude oil from water. DES concentration is also an important parameter that decides the absorption capacity of MS. Too high a concentration of the impregnating solution and consequently too much-impregnating material may clog the pores and reduce the absorption capacity. In addition, too much DES after extrusion can cause DES to enter the pus and make it impossible to reuse it. On the other hand, too low a concentration of DES may cause uneven distribution on the surface of the sponge and result in a lack of selectivity in the process of absorbing oil from water. The obtained results indicate that 15% of the DES solution is an optimum parameter. Lower and higher DES concentrations provide to reduce the absorption capacity of both model and real crude oil. In addition, it can be observed that the absorption equilibrium was reached after 37 sec of immersion. The shorter time meant that the sponge was unable to absorb the oil into all open pores.

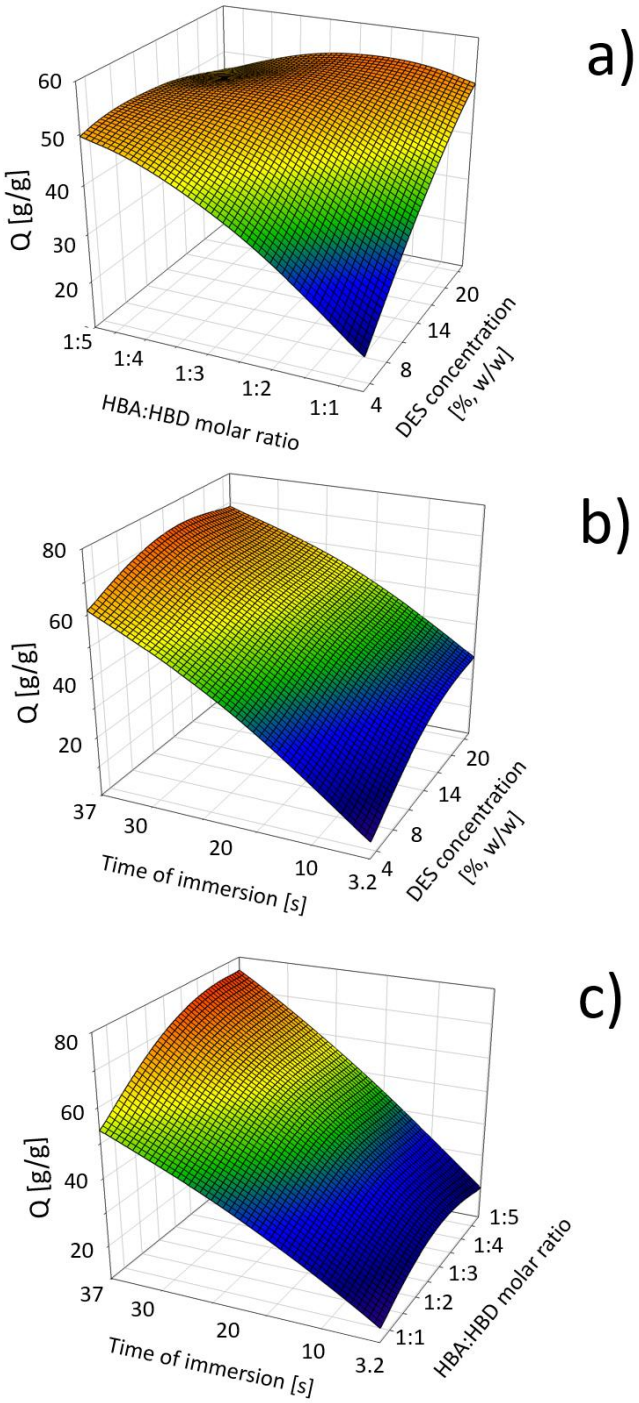

558

559 **Figure 5** Response surface plots for real crude oil (CO_3) surface area dependence on: a)
560 HBA:HBD molar ratio and DES concentration, b) time of immersion and DES concentration, c)
561 time of immersion and HBA:HBD molar ratio.

562 3.4.2. Application of MS-DES for absorption of various type of crude oil

563

564 In the further part of the studies, various types of crude oils were absorbed by MS-E:M (1:5) under
565 optimal conditions. The results are presented in Figure 14, and S3. The obtained results indicate
566 that a higher absorption capacity was observed for both relatively light models and real crude oils.
567 The absorption capacity were 99.8, 102.4, 126.1, and 118 g/g for CO_1, CO_2, MCO_1, and
568 M_CO2, respectively. It can be obtained that with the increase in the content of heavier
569 components i.e. resins, and asphaltenes, the MS-E:M (1:5) sorption capacity gradually decreases.
570 This is probably due to the fact that the components with more complex structures have limited
571 access to active sites on the sponge surface, capable of forming strong bonds. In addition, they
572 cover active sites for substances with smaller structures that could more easily attach to the
573 impregnating layer. However, the differences in the absorption capacities of different types of
574 crude oil are very small, so it can be concluded that the sponge can be used with great efficiency
575 to remove different types of crude oil from the water surface. The largest differences in absorption
576 capacities can be observed between the model and real crude oils. In the case of model crude oil,
577 higher absorption capacities were obtained. This is due to the significantly lower amount of
578 substances contained in model mixtures. The same trend has also been observed in other works
579 [61].

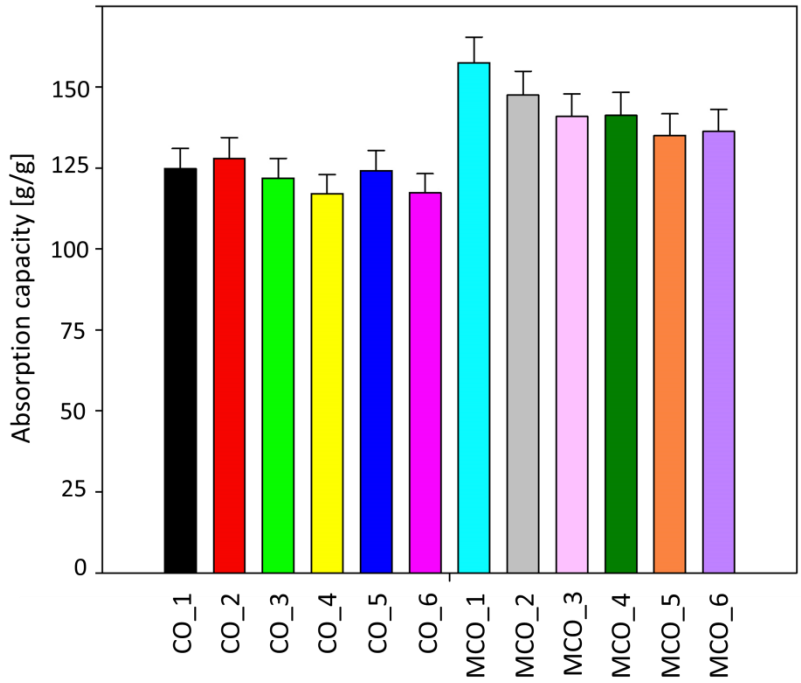

Figure 6 Absorption capacity of various types of real and mode crude oils using MS-E:M (1:5).

In order to deep insight into the selected group of crude oils absorption by MS-E:M (1:5), the TLC-FID studies were prepared. Both model and real crude oils groups were analyzed before and after the absorption and squeezing process using the TLC-FID technique (Figure 15 and Table 3). The results indicate that only small differences can be obtained in each crude oil sample before and after the absorption process. The highest differences were observed for real crude oil samples. However, these differences do not excite 2.6 %, w/w which is in the range of error. The results indicate that crude oil after removal from water does not change compositions. In addition, the lack of changes in S, and Ar concentration in crude oil samples indicate that DES does not make it into crude oil. This indicates that the crude oil can be used for further processing and does not need to be disposed of, which has significant financial benefits.

Table 2 Composition of the crude oil samples before and after squeezing.

Crude oil sample	S (%, w/w) ± SD		Ar (%, w/w) ± SD		R (%, w/w) ± SD		A (%, w/w) ± SD	
	Pure CO	CO After squeezing	Pure CO	CO After squeezing	Pure CO	CO After squeezing	Pure CO	CO After squeezing
CO_1	70.8 ± 3.7	70.2 ± 3.6	24.2 ± 1.1	23.9 ± 1.2	4.8 ± 0.2	4.9 ± 0.2	0.2 ± 0.01	1 ± 0.05
CO_2	72 ± 4.1	71.6 ± 3.4	22.3 ± 1.1	21.8 ± 1.1	5.0 ± 0.3	5.2 ± 0.3	0.7 ± 0.03	1.4 ± 0.07
CO_3	62.1 ± 3.2	61.2 ± 2.8	19.8 ± 1	19.4 ± 0.9	14.7 ± 0.8	14.8 ± 0.7	3.4 ± 0.2	4.6 ± 0.23
CO_4	72.3 ± 3.8	71.8 ± 3.7	18.2 ± 0.8	18.0 ± 1.0	8.1 ± 0.4	8.5 ± 0.4	1.4 ± 4.3	1.7 ± 0.09
CO_5	39.9 ± 2.2	39.8 ± 2.1	24.9 ± 1	24.6 ± 1.2	30.9 ± 1.7	31.2 ± 1.6	4.3 ± 0.24	4.4 ± 0.22
CO_6	28.1 ± 1.1	28.9 ± 1.6	29.9 ± 1.1	27.9 ± 1.5	32.7± 1.8	33.6 ± 1.7	10.2 ± 0.56	7.6 ± 0.39
MCO_1	80 ± 4.4	79.4 ± 3.7	10 ± 0.4	9.8 ± 0.5	9.5 ± 0.5	9.9 ± 0.5	0.5 ± 0.03	0.9 ± 0.05
MCO_2	70 ± 3.4	69.1 ± 2.8	20 ± 1.2	19.9 ± 1	9.5 ± 0.5	10.2 ± 0.5	0.5 ± 0.03	0.8 ± 0.04
MCO_3	50 ± 2.4	49.7 ± 2.4	30 ± 1.2	30.8 ± 1.6	19.5 ± 1.1	19.4 ± 1	0.5 ± 0.03	0.1 ± 0.005
MCO_4	40 ± 1.9	39.2 ± 2.0	50 ± 2.1	50.1 ± 2.6	9.5 ± 0.5	9.9 ± 0.5	0.5 ± 0.03	0.8 ± 0.04
MCO_5	20 ± 1.0	19.3 ± 0.9	40 ± 1.9	41.0 ± 2	38.6 ± 1.8	39.8 ± 2.1	1 ± 0.06	1.3 ± 0.07
MCO_6	10 ± 0.5	9.4 ± 0.5	50 ± 2.1	49.7 ± 2.4	39 ± 2.1	40.7 ± 2.2	1 ± 0.06	0.2 ± 0.01

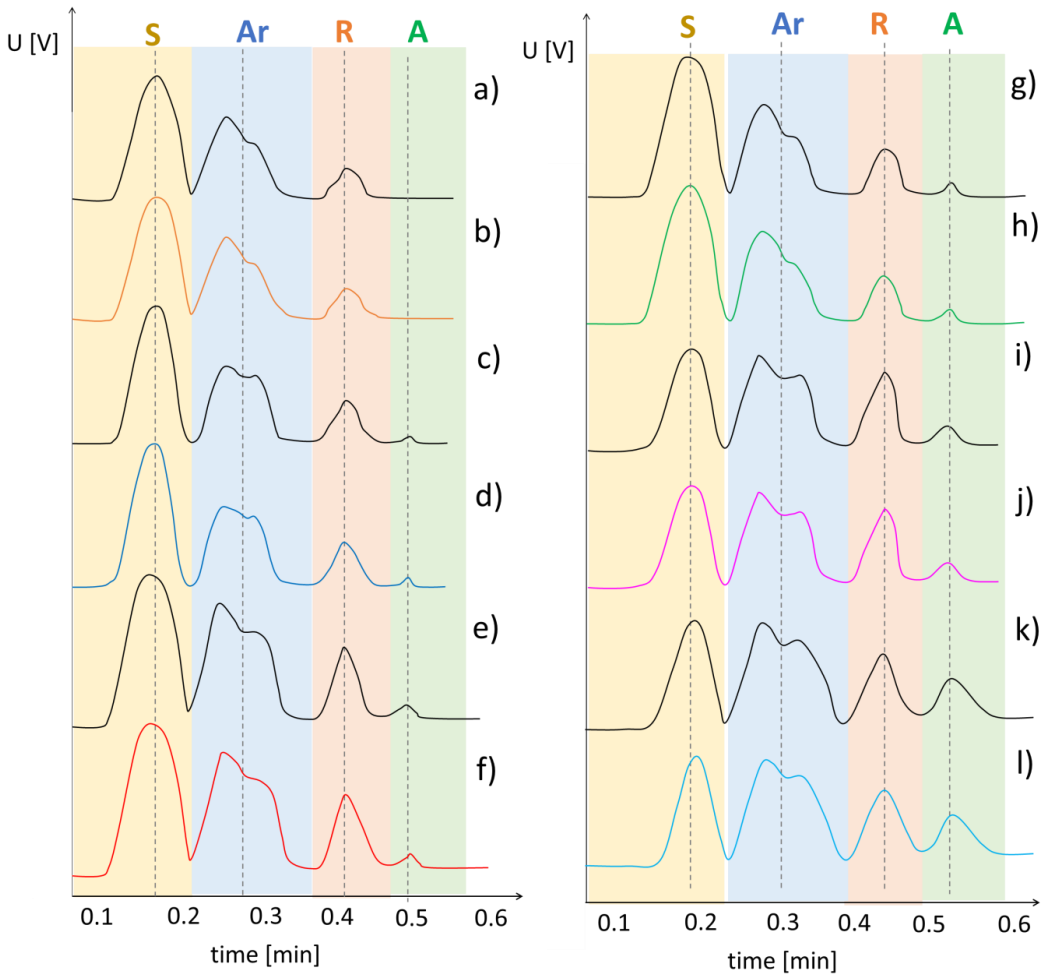

596

597 **Figure 7** TLC-FID chromatograms of real crude oil before (black line) and after absorption and
598 squeezing process (color lines) a-b) CO_1; c-d) CO_2; e-f) CO_3; g-h) CO_4; i-j) CO_5; k-l)
599 CO_5.

600 3.4.3. Reusability

601 Reusability is one of the most important parameters that determine the cost of processes. In these
602 studies, MS-E:M (1:5) was immersed in the real crude oil sample (CO_3) for one minute and then
603 the sponge was taken out and squeezed in order to remove crude oil. In the next step, the sponge
604 was dried at 60 °C for 0.5 hours. Sponge after crude oil absorption and after crude oil removal was
605 weighted. This procedure was repeated 80 times. The obtained results are presented in Figure 16.

606 The obtained results show that the sponges do not change their absorption capacity even after 80
607 cycles.

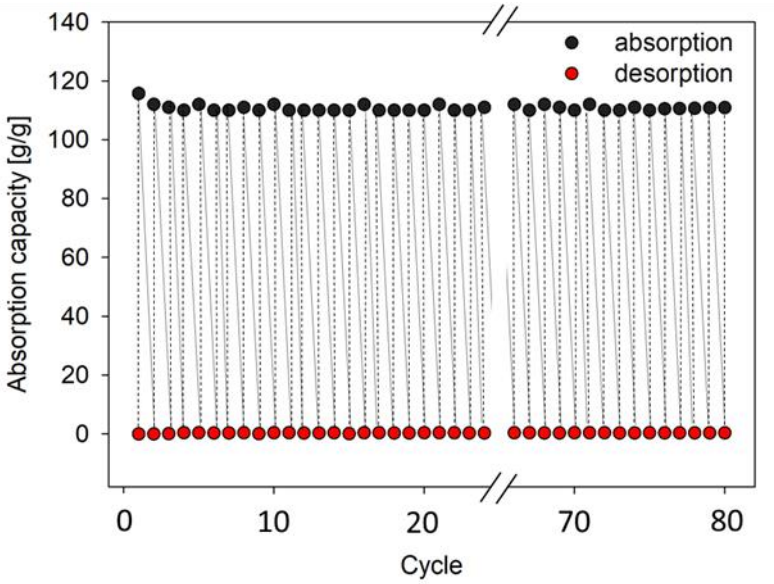

608

609 **Figure 8** Absorption – desorption reusability cycles of MS-E:M (1:5) for real crude oil sample
610 (CO_3).

611 3.4.4. Comparison of prepared MS-DES with other studies

612 The MS-E:M (1:5) was compared with literature data of other superhydrophobic sponges.
613 However, there are only a few studies of the real crude oil absorption capacity of sponges. Most
614 of the presented works include only results of pure solvents' absorption, which do not relate to very
615 complex crude oil mixtures. A comparison of real crude oil absorption capacity for sponges with
616 different functionalities is presented in Table 4. The results indicate that new MS-DES show higher
617 crude oil absorption capacity than most of the sponges. The water contact angle is comparable to
618 the literature data. Some presented studies required higher surface temperature, which can
619 improved absorption capacity, and selectivity of sponges. However, this increases the energy
620 requirement and thus increases the cost of the entire process. In addition, the possibility of multiple

regenerations is a decisive competitive advantage of the new MS in comparison with other sponges.

Table 4 Comparison of real crude oil absorption capacity for sponges with different functionalities

Type of sponge	Absorption capacity [g/g]	Surface temperature	Water contact angle [°]	Regeneration cycles	Literature
UIO-66-F4@rGO/MS	61	RT	155	10	[62]
MoS2-RS	15-67	76	151	100	[63]
MF/rGO	140.7	92.4	136.8	10	[64]
PDMS/CuS/PDA@MF	117	86.7	169.3	-	[65]
CNT/PDMS-PU	140.7	88	154	-	[66]
TiO_2/PDA@MF	11.2	90.7	151	5	[67]
PU	36.3	RT	45	-	[68]
FGN/PU	44.1	RT	160	50	[68]
UMS-3	83.0	RT	131	30	[61]
MS-E:M (1:5)	96.1 – 132.2	RT	152	80	This studies

4. Conclusions

In the studies, a new superhydrophobic and superolephilic melamine sponges based on deep eutectic solvents were prepared, characterized, and used for the process of model and real crude oil removal from water. Due to the fact that the new sponges have to be used in the environmental waters i.e. sea or ocean, all the tested impregnation layers were composed only of natural components including terpenes, phenols, and carboxylic acids. The most important parameters that

631 determine the selection of a suitable DES as an impregnating layer were high affinity to the crude
632 oil components and low affinity to water. Based on COSMO-RS preselection, only DES composed
633 of monoterpenes, and linear carboxylic acids met the requirements of suitable impregnation
634 materials. From the wide range of tested melamine sponges impregnated by DES, the MS-E:M
635 (1:5) showed the most favorable properties i.e. superhydrophobic contact angle of 152°,
636 superoleophilic contact angle of 0°, low density of 9.23 mg/cm^3, high porosity of 99.39%,
637 relatively high crude oil absorption capacity in the range of 96.1 – 132.2 g/g which only slightly
638 depends on crude oil compositions, excellent reusability which is almost not changing even after
639 80 cycles.

640 The proposed impregnation method with DES, which is cheap, easy, and environmental-
641 friendly, can be used for surface modification of almost all types of new or waste sponges.
642 Therefore, it can be conducted that sponges coated by DES are promising sorbents for crude oil
643 spill containment and environmental remediation.

644 **FUNDING SOURCES**

645 The research is funded by National Science Centre, Poland within the grant project (no. DEC-
646 2020/04/X/ST8/00754).

647 **NOTES**

648 The authors declare no competing financial interest.

649

650 **References**

651 [1] L.J. Fernandes, A.P. Barbosa-Póvo, S. Relvas, Risk management framework for the

petroleum supply chain, Comput. Aided Chem. Eng. 28 (2010) 157–162. https://doi.org/10.1016/S1570-7946(10)28027-6.

[2] R. Almeda, C. Hyatt, E.J. Buskey, Toxicity of dispersant Corexit 9500A and crude oil to marine microzooplankton, Ecotoxicol. Environ. Saf. 106 (2014) 76–85. https://doi.org/10.1016/j.ecoenv.2014.04.028.

[3] J.B.C. Jackson, J.D. Cubit, B.D. Keller, V. Batista, K. Burns, H.M. Caffey, R.L. Caldwell, S.D. Garrity, C.D. Getter, C. Gonzalez, H.M. Guzman, K.W. Kaufmann, A.H. Knap, S.C. Levings, M.J. Marshall, R. Steger, R.C. Thompson, E. Weil, Ecological effects of a major oil spill on Panamanian coastal marine communities, Science (80-.). 243 (1989) 37–44. https://doi.org/10.1126/science.243.4887.37.

[4] E.B. Kujawinski, M.C.K. Soule, D.L. Valentine, A.K. Boysen, K. Longnecker, M.C. Redmond, Fate of Dispersants Associated with the Deepwater Horizon Oil Spill, Environ. Sci. Technol. 45 (2011) 1–9. https://doi.org/10.1021/es103838p.

[5] V. Broje, A.A. Keller, Improved mechanical oil spill recovery using an optimized geometry for the skimmer surface, Environ. Sci. Technol. 40 (2006) 7914–7918. https://doi.org/10.1021/es061842m.

[6] L. Buist, J. McCourt, S. Potter, S. Ross, K. Trudel, In situ burning, Pure Appl. Chem. 71 (1999) 43–65. https://doi.org/10.1351/pac199971010043.

[7] J. Ge, H.Y. Zhao, H.W. Zhu, J. Huang, L.A. Shi, S.H. Yu, Advanced Sorbents for Oil-Spill Cleanup: Recent Advances and Future Perspectives, Adv. Mater. 28 (2016) 10459–10490. https://doi.org/10.1002/adma.201601812.

673 [8] R.R. Lessard, G. DeMarco, The significance of oil spill dispersants, in: Spill Sci. Technol.
674 Bull., Pergamon, 2000: pp. 59–68. https://doi.org/10.1016/S1353-2561(99)00061-4.

675 [9] A.D. Venosa, X. Zhu, Biodegradation of crude oil contaminating marine shorelines and
676 freshwater wetlands, Spill Sci. Technol. Bull. 8 (2003) 163–178.
677 https://doi.org/10.1016/S1353-2561(03)00019-7.

678 [10] L. Bandura, M. Franus, G. Józefaciuk, W. Franus, Synthetic zeolites from fly ash as
679 effective mineral sorbents for land-based petroleum spills cleanup, Fuel. 147 (2015) 100–
680 107. https://doi.org/10.1016/j.fuel.2015.01.067.

681 [11] Y. Lu, Z. Niu, W. Yuan, Multifunctional magnetic superhydrophobic carbonaceous aerogel
682 with micro/nano-scale hierarchical structures for environmental remediation and energy
683 storage, Appl. Surf. Sci. 480 (2019) 851–860. https://doi.org/10.1016/j.apsusc.2019.03.060.

684 [12] C. Wang, S. Yang, Q. Ma, X. Jia, P.C. Ma, Preparation of carbon nanotubes/graphene
685 hybrid aerogel and its application for the adsorption of organic compounds, Carbon N. Y.
686 118 (2017) 765–771. https://doi.org/10.1016/j.carbon.2017.04.001.

687 [13] C. Teas, S. Kalligeros, F. Zanikos, S. Stournas, E. Lois, G. Anastopoulos, Investigation of
688 the effectiveness of absorbent materials in oil spills clean up, Desalination. 140 (2001) 259–
689 264. https://doi.org/10.1016/S0011-9164(01)00375-7.

690 [14] O.S.H. Santos, M. Coelho da Silva, V.R. Silva, W.N. Mussel, M.I. Yoshida, Polyurethane
691 foam impregnated with lignin as a filler for the removal of crude oil from contaminated
692 water, J. Hazard. Mater. 324 (2017) 406–413.
693 https://doi.org/10.1016/j.jhazmat.2016.11.004.

[15] M. Khosravi, S. Azizian, R. Boukherroub, Efficient oil/water separation by superhydrophobic CuxS coated on copper mesh, Sep. Purif. Technol. 215 (2019) 573–581. https://doi.org/10.1016/j.seppur.2019.01.039.

[16] A. Xie, J. Cui, Y. Chen, J. Lang, C. Li, Y. Yan, J. Dai, Capillarity-driven both light and heavy oil/water separation via combined system of opposite superwetting meshes, Sep. Purif. Technol. 215 (2019) 1–9. https://doi.org/10.1016/j.seppur.2018.12.075.

[17] P. Phanthong, P. Reubroycharoen, S. Kongparakul, C. Samart, Z. Wang, X. Hao, A. Abudula, G. Guan, Fabrication and evaluation of nanocellulose sponge for oil/water separation, Carbohydr. Polym. 190 (2018) 184–189. https://doi.org/10.1016/j.carbpol.2018.02.066.

[18] R.G. Toro, P. Calandra, F. Federici, T. de Caro, A. Mezzi, B. Cortese, A.L. Pellegrino, G. Malandrino, D. Caschera, Development of superhydrophobic, self-cleaning, and flame-resistant DLC/TiO2 melamine sponge for application in oil–water separation, J. Mater. Sci. 55 (2020) 2846–2859. https://doi.org/10.1007/s10853-019-04211-2.

[19] J. Chen, H. You, L. Xu, T. Li, X. Jiang, C.M. Li, Facile synthesis of a two-tier hierarchical structured superhydrophobic-superoleophilic melamine sponge for rapid and efficient oil/water separation, J. Colloid Interface Sci. 506 (2017) 659–668. https://doi.org/10.1016/j.jcis.2017.07.066.

[20] E.K. Sam, J. Liu, X. Lv, Surface engineering materials of superhydrophobic sponges for oil/water separation: A review, Ind. Eng. Chem. Res. 60 (2021) 2353–2364. https://doi.org/10.1021/acs.iecr.0c05906.

[21] E.A. Pavlatou, Commercial Sponges as A Novel Technology for Crude Oil Removal from Seawater and Industrial Wastewater: A Review, Biomed. J. Sci. Tech. Res. 25 (2020) 19426–19436. https://doi.org/10.26717/bjstr.2020.25.004251.

[22] S. Mukherjee, S. Sharma, S.K. Ghosh, Hydrophobic metal-organic frameworks: Potential toward emerging applications, APL Mater. 7 (2019) 1–14. https://doi.org/10.1063/1.5091783.

[23] Y. Chen, T. Mu, Revisiting greenness of ionic liquids and deep eutectic solvents, Green Chem. Eng. 2 (2021) 174–186. https://doi.org/10.1016/j.gce.2021.01.004.

[24] M. González-Miquel, I. Díaz, Green solvent screening using modeling and simulation, Curr. Opin. Green Sustain. Chem. 29 (2021) 100469. https://doi.org/10.1016/j.cogsc.2021.100469.

[25] X. Chen, J.A. Weibel, S. V. Garimella, Continuous Oil-Water Separation Using Polydimethylsiloxane-Functionalized Melamine Sponge, Ind. Eng. Chem. Res. 55 (2016) 3596–3602. https://doi.org/10.1021/acs.iecr.6b00234.

[26] Y. Feng, Y. Wang, Y. Wang, J. Yao, Furfuryl alcohol modified melamine sponge for highly efficient oil spill clean-up and recovery, J. Mater. Chem. A. 5 (2017) 21893–21897. https://doi.org/10.1039/c7ta06966a.

[27] H. Liu, S. Su, J. Xie, Y. Ma, C. Tao, Preparation of superhydrophobic magnetic stearic acid polyurethane sponge for oil-water separation, J. Mater. Res. 35 (2020) 2925–2935. https://doi.org/10.1557/jmr.2020.260.

[28] C.G. Yoo, Y. Pu, A.J. Ragauskas, Ionic liquids: Promising green solvents for lignocellulosic

biomass utilization, Curr. Opin. Green Sustain. Chem. 5 (2017) 5–11. https://doi.org/10.1016/j.cogsc.2017.03.003.

[29] L.A. Blanchard, D. Hancu, E.J. Beckman, J.F. Brennecke, Green processing using ionic liquids and CO2, Nature. 399 (1999) 28–29. www.nature.com.

[30] A. Romero, A., Santos, A., Tojo, J. & Rodríguez, Toxicity and biodegradability of imidazolium ionic liquids, J. Hazard. Mater. 151 (2008) 268–273. https://doi.org/10.1016/J.JHAZMAT.2007.10.079.

[31] J. Cao, E. Su, Hydrophobic deep eutectic solvents: the new generation of green solvents for diversified and colorful applications in green chemistry, J. Clean. Prod. 314 (2021) 127965. https://doi.org/10.1016/j.jclepro.2021.127965.

[32] M.A. Alam, G. Muhammad, M.N. Khan, M. Mofijur, Y. Lv, W. Xiong, J. Xu, Choline chloride-based deep eutectic solvents as green extractants for the isolation of phenolic compounds from biomass, J. Clean. Prod. 309 (2021) 127445. https://doi.org/10.1016/j.jclepro.2021.127445.

[33] P. Makoś, E. Słupek, J. Gębicki, Hydrophobic deep eutectic solvents in microextraction techniques–A review, Microchem. J. 152 (2020). https://doi.org/10.1016/j.microc.2019.104384.

[34] P. Makoś, A. Przyjazny, G. Boczkaj, Hydrophobic deep eutectic solvents as “green” extraction media for polycyclic aromatic hydrocarbons in aqueous samples, J. Chromatogr. A. 1570 (2018) 28–37. https://doi.org/10.1016/j.chroma.2018.07.070.

[35] P. Makoś, E. Słupek, J. Gębicki, Extractive detoxification of feedstocks for the production

of biofuels using new hydrophobic deep eutectic solvents – Experimental and theoretical studies, J. Mol. Liq. 308 (2020) 113101–113112. https://doi.org/10.1016/j.molliq.2020.113101.

[36] P. Makoś, G. Boczkaj, Deep eutectic solvents based highly efficient extractive desulfurization of fuels – Eco-friendly approach, J. Mol. Liq. 296 (2019) 111916–111927. https://doi.org/10.1016/j.molliq.2019.111916.

[37] E. Słupek, P. Makoś-Chełstowska, J. Gębicki, Removal of siloxanes from model biogas by means of deep eutectic solvents in absorption process, Materials (Basel). 14 (2021) 1–20. https://doi.org/10.3390/ma14020241.

[38] E. Słupek, P. Makoś, J.Gębicki, Deodorization of model biogas by means of novel non-ionic deep eutectic solvent, Arch. Environ. Prot. 46 (2020) 41–46. https://doi.org/10.24425/aep.2020.132524.

[39] E. Słupek, P. Makoś, Absorptive Desulfurization of Model Biogas Stream Using Choline Chloride-Based Deep Eutectic Solvents, Sustainability. 12 (2020) 1619–1635. https://doi.org/10.3390/su12041619.

[40] E. Słupek, P. Makoś, J. Gębicki, Theoretical and Economic Evaluation of Low-Cost Deep Eutectic Solvents for Effective Biogas Upgrading to Bio-Methane, Energies. 13 (2020) 3379. https://doi.org/10.3390/en13133379.

[41] P. Makoś-Chełstowska, E. Słupek, J. Gębicki, Deep eutectic solvents – based green absorbents for effective volatile organochlorine compounds removal from biogas, Green Chem. (2021). https://doi.org/10.1039/d1gc01735g.

[42] A. Roda, A.A. Matias, A. Paiva, A.R.C. Duarte, Polymer science and engineering using deep eutectic solvents, Polymers (Basel). 11 (2019) 1–22. https://doi.org/10.3390/polym11050912.

[43] M. Jablonský, A. Škulcová, J. Šima, Use of deep eutectic solvents in polymer chemistry–a review, Molecules. 24 (2019) 1–33. https://doi.org/10.3390/molecules24213978.

[44] P. Makoś, E. Słupek, A. Małachowska, Silica Gel Impregnated by Deep Eutectic Solvents for Adsorptive Removal of BTEX from Gas Streams, Materials (Basel). 13 (2020) 1894. https://doi.org/10.3390/ma13081894.

[45] M.T. Donato, R. Colaço, L.C. Branco, B. Saramago, A review on alternative lubricants: Ionic liquids as additives and deep eutectic solvents, J. Mol. Liq. 333 (2021) 116004. https://doi.org/10.1016/j.molliq.2021.116004.

[46] A.E. Ünlü, A. Arlkaya, S. Takaç, Use of deep eutectic solvents as catalyst: A mini-review, Green Process. Synth. 8 (2019) 355–372. https://doi.org/10.1515/gps-2019-0003.

[47] N. Gissawong, S. Mukdasai, S. Boonchiangma, S. Sansuk, S. Srijaranai, A rapid and simple method for the removal of dyes and organophosphorus pesticides from water and soil samples using deep eutectic solvent embedded sponge, Chemosphere. 260 (2020) 127590. https://doi.org/10.1016/j.chemosphere.2020.127590.

[48] P. Makoś-Chełstowska, E. Słupek, A. Kramarz, J. Gębicki, New Carvone-Based Deep Eutectic Solvents for Siloxanes Capture from Biogas, Int. J. Mol. Sci. 22 (2021) 9551–9574.

[49] A. Zielińska-Jurek, Z. Bielan, S. Dudziak, I. Wolak, Z. Sobczak, T. Klimczuk, G. Nowaczyk, J. Hupka, Design and application of magnetic photocatalysts for water

799 treatment. The effect of particle charge on surface functionality, Catalysts. 7 (2017).
800 https://doi.org/10.3390/catal7120360.

801 [50] Y. Ding, W. Xu, Y. Yu, H. Hou, Z. Zhu, One-Step Preparation of Highly Hydrophobic and
802 Oleophilic Melamine Sponges via Metal-Ion-Induced Wettability Transition, ACS Appl.
803 Mater. Interfaces. 10 (2018) 6652–6660. https://doi.org/10.1021/acsami.7b13626.

804 [51] IP 469: Determination of saturated, aromatic and polar compounds in petroleum products
805 by thin layer chromatography and flame ionization detection | EI - Publishing, (2006).
806 https://publishing.energyinst.org/ip-test-methods/full-list-of-ip-test-methods-
807 publications/ip-469-determination-of-saturated,-aromatic-and-polar-compounds-in-
808 petroleum-products-by-thin-layer-chromatography-and-flame-ionization-detection
809 (accessed September 3, 2021).

810 [52] J. Han, C. Dai, G. Yu, Z. Lei, Parameterization of COSMO-RS model for ionic liquids,
811 Green Energy Environ. 3 (2018) 247–265.
812 https://doi.org/https://doi.org/10.1016/j.gee.2018.01.001.

813 [53] V. Migliorati, F. Sessa, P. D'Angelo, Deep eutectic solvents: A structural point of view on
814 the role of the cation, Chem. Phys. Lett. X. 2 (2019) 100001.
815 https://doi.org/10.1016/j.cpletx.2018.100001.

816 [54] Z. Li, Z. Guo, Flexible 3D porous superhydrophobic composites for oil-water separation
817 and organic solvent detection, Mater. Des. 196 (2020) 109144.
818 https://doi.org/10.1016/J.MATDES.2020.109144.

819 [55] Y. Zhou, Y. Wang, T. Liu, G. Xu, G. Chen, H. Li, L. Liu, Q. Zhuo, J. Zhang, C. Yan,

820 Superhydrophobic hBN-Regulated Sponges with Excellent Absorbency Fabricated Using a
821 Green and Facile Method, Sci. Rep. 7 (2017) 1–10. https://doi.org/10.1038/srep45065.

822 [56] Y. Zhang, Q. Pan, G. Chai, M. Liang, G. Dong, Q. Zhang, J. Qiu, Synthesis and
823 luminescence mechanism of multicolor-emitting g-C3N4 nanopowders by low temperature
824 thermal condensation of melamine, Sci. Rep. 3 (2013) 1–8.
825 https://doi.org/10.1038/srep01943.

826 [57] V.H. Pham, J.H. Dickerson, Superhydrophobic silanized melamine sponges as high
827 efficiency oil absorbent materials, ACS Appl. Mater. Interfaces. 6 (2014) 14181–14188.
828 https://doi.org/10.1021/am503503m.

829 [58] A. Stolz, S. Le Floch, L. Reinert, S.M.M. Ramos, J. Tuaillon-Combes, Y. Soneda, P.
830 Chaudet, D. Baillis, N. Blanchard, L. Duclaux, A. San-Miguel, Melamine-derived carbon
831 sponges for oil-water separation, Carbon N. Y. 107 (2016) 198–208.
832 https://doi.org/10.1016/j.carbon.2016.05.059.

833 [59] P.J. Larkin, M.P. Makowski, N.B. Colthup, The form of the normal modes of s-triazine:
834 infrared and Raman spectral analysis and ab initio force field calculations, Spectrochim.
835 Acta Part A Mol. Biomol. Spectrosc. 55 (1999) 1011–1020. https://doi.org/10.1016/S1386-
836 1425(98)00244-3.

837 [60] X. Wu, Y. Tao, Y. Lu, L. Dong, Z. Hu, High-pressure pyrolysis of melamine route to
838 nitrogen-doped conical hollow and bamboo-like carbon nanotubes, Diam. Relat. Mater. 15
839 (2006) 164–170. https://doi.org/10.1016/J.DIAMOND.2005.09.018.

840 [61] Y. Fang, L. Yan, H. Liu, Facile Preparation of Hydrophobic Melamine Sponges using

Naturally Derived Urushiol for Efficient Oil/Water Separation, ACS Appl. Polym. Mater. 2 (2020) 3781–3788. https://doi.org/10.1021/acsapm.0c00393.

[62] Y. Zhan, S. He, J. Hu, S. Zhao, G. Zeng, M. Zhou, G. Zhang, A. Sengupta, Robust super-hydrophobic/super-oleophilic sandwich-like UIO-66-F4@rGO composites for efficient and multitasking oil/water separation applications, Elsevier B.V., 2020. https://doi.org/10.1016/j.jhazmat.2019.121752.

[63] M. Yu, P. Xu, J. Yang, L. Ji, C. Li, Self-Growth of MoS2 Sponge for Highly Efficient Photothermal Cleanup of High-Viscosity Crude Oil Spills, Adv. Mater. Interfaces. 7 (2020) 1–10. https://doi.org/10.1002/admi.201901671.

[64] Y. Wang, L. Zhou, X. Luo, Y. Zhang, J. Sun, X. Ning, Y. Yuan, Solar-heated graphene sponge for high-efficiency clean-up of viscous crude oil spill, J. Clean. Prod. 230 (2019) 995–1002. https://doi.org/10.1016/j.jclepro.2019.05.178.

[65] H. Niu, J. Li, X. Wang, F. Luo, Z. Qiang, J. Ren, Solar-Assisted, Fast, and in Situ Recovery of Crude Oil Spill by a Superhydrophobic and Photothermal Sponge, ACS Appl. Mater. Interfaces. 13 (2021) 21175–21185. https://doi.org/10.1021/acsami.1c00452.

[66] J. Chang, Y. Shi, M. Wu, R. Li, L. Shi, Y. Jin, W. Qing, C. Tang, P. Wang, Solar-assisted fast cleanup of heavy oil spills using a photothermal sponge, J. Mater. Chem. A. 6 (2018) 9192–9199. https://doi.org/10.1039/c8ta00779a.

[67] J. Yang, P. Xu, Y. Yao, Y. Li, B. Shi, X. Jia, H. Song, A solar-heated Janus sponge with excellent floating stability for efficient cleanup of heavy oil, Mater. Des. 195 (2020) 108979. https://doi.org/10.1016/j.matdes.2020.108979.

[68] S. Zhou, G. Hao, X. Zhou, W. Jiang, T. Wang, N. Zhang, L. Yu, One-pot synthesis of robust superhydrophobic, functionalized graphene/polyurethane sponge for effective continuous oil-water separation, Chem. Eng. J. 302 (2016) 155–162. https://doi.org/10.1016/j.cej.2016.05.051.